CHEMISTRY OF MATERIALS

pubs.acs.org/cm

Perspective

Advances and Challenges of Hydrogel Materials for Robotic and Sensing Applications

Yi Ouyang, Gaoshan Huang, Jizhai Cui, Hong Zhu, Guanghui Yan, and Yongfeng Mei*

Cite This: *Chem. Mater.* 2022, 34, 9307−9328

Read Online

ACCESS | Metrics & More | Article Recommendations

ABSTRACT: Hydrogels are soft materials composed of a three-dimensional (3D) hydrophilic polymer network filled with a large amount of water. Different from rigid machines, hydrogel-based robots are encoded with energy conversion mechanisms that allow sensing, adaption, transformation, and response in complex environments. In this perspective, we discuss the advances and challenges of hydrogel materials for soft robotic and sensing applications. In the first part, we introduce stimuli-responsive hydrogel sensors that can receive external energy inputs from different stimuli and translate them into in the geometrical, optical, electrical, and biological output signals. Then, we comprehensively discuss the recent development of hydrogel robot systems that exploit the responsive properties to achieve diverse locomotion models and functions. On the basis of the distinct driving force and locomotion mechanisms, we categorize hydrogel robots into two main kinds: one is the active robot that deforms by stimuli-responsive swelling of soft hydrogels, and the other is the passive motor that is propelled by reactive matters. We compare the advantages and challenges of each strategy and show how to transform biomimetic principles into technological capabilities through material and structural designs. We finally provide a critical perspective on the key challenges in the integration of functionality in hydrogel robotic systems and reasonable directions to push hydrogel robots toward diverse applications.

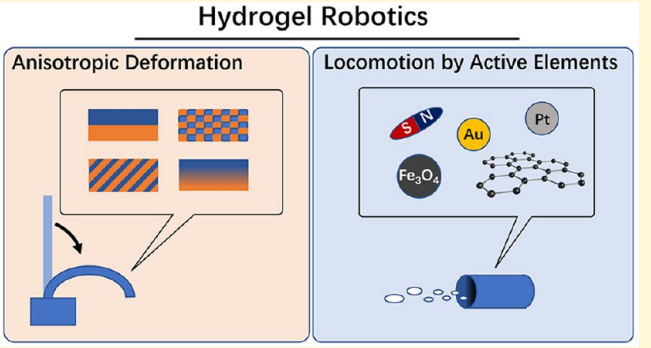

1. INTRODUCTION

The recent development of miniaturized robots toward healthcare and biomedical applications has drawn great attention from both mechanicians and materials scientists.[1,2] Traditional rigid machines have come to a bottleneck where the combination of motors, the power source, logic circuits, and computational elements cannot be easily miniaturized to satisfy the increasing demand for *in vivo* applications.[3−5] On the other hand, stimuli-responsive soft materials can translate external energy into mechanical forces and deformations, which provides a promising alternative to integrate on-board sensing and deformation capabilities into miniaturized soft robots. Since the proposal of the hydrophilic copolymer polyhydroxyethyl methacrylate (pHEMA) for permanent contact applications with biological tissues in 1960s,[6] hydrogels have been regarded as the most prominent materials in bioengineering due to their biocompatibility, low modulus, and permeability to nutrients and metabolites.[7] Hydrogel is a three-dimensional (3D) hydrophilic network containing a large amount of aqueous solutions.[8] Due to their physically or chemically cross-linked polymer structure, hydrogels exhibit the properties of elastic solids with deformability and softness. Furthermore, the high content of water within the networks brings them fluid-like properties, such as the transparency of light and the permeability of ions and molecules.[1,9] Due to their unique properties, the application of hydrogels expands from bioengineering,[10,11] drug delivery,[12] and microfluidics[13−15] to soft robotics[16,17] and integrated senors.[9]

Hydrogel materials with stimuli-responsive properties could be the key elements that enable the integration of sensing, actuation, and locomotion in intelligent soft robots. The joint efforts made by the discovery of materials and the optimization of the robot's design have significantly enriched motion mechanisms, constructed structures, and functional tasks of hydrogel robots. Generally, hydrogel robots can be classified into two main kinds: one is an active hydrogel soft robot that deforms by stimuli-responsive swelling, and the other is a passive motor that is propelled by other reactive substances embedded in the hydrogels (Figure 1).

Received: June 30, 2022
Revised: September 23, 2022
Published: October 18, 2022

https://doi.org/10.1021/acs.chemmater.2c01960
Chem. Mater. 2022, 34, 9307−9328

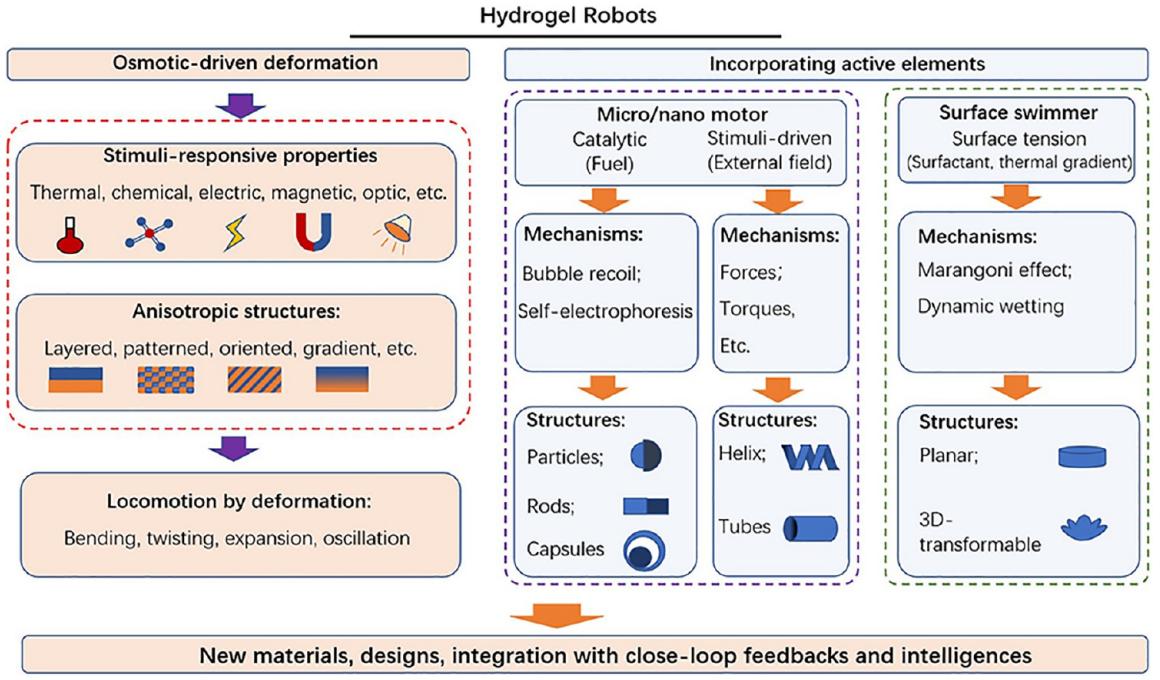

Figure 1. Hydrogel robots with diverse mechanisms, structures, and functions.

In nature, plants utilize the flow of water to realize their particular movements.[18,19] The motions are caused by their uniquely oriented cellulose structures.[8,20] Inspired by plants, the osmotic pressure-driven hydrogel soft robots adopted layered, patterned, or oriented structures to perform anisotropic deformations in response to external stimuli, such as light,[21−24] an electric field,[25] temperature,[26,27] ionic strength,[28] or a magnetic field.[29−32] The utilization of anisotropic structures or nonuniform distribution of external fields enables hydrogel robots to achieve bending,[33] twisting,[34] expansion,[24] and oscillation deformations.[35,36] The hydrogel robots constructed by such mechanisms can be defined as the active soft robots.

On the other hand, when active elements are incorporated into hydrogel matrices, hydrogel motors are micromachines that are passively powered by the catalytic decomposition of biochemical fuels or driven by external fields. The term "passive" refers to the fact that these hydrogel micromachines do not involve the osmotic-driven swelling of the hydrogel itself.[37] Most catalytic hydrogel motors move autonomously in liquid environments by catalytic bubble recoil, and the propulsion directions are predetermined by the structural anisotropy. One can also apply external fields to steer the movements of the motors. For example, it is a feasible approach to exert force or torque on the motor by applying a magnetic field[38] or to accelerate the catalytic reactions by applying near-infrared light (NIR) illumination.[39]

Moreover, there is another type of new hydrogel motors that are capable of various agile autonomous locomotion on water surfaces through the manipulation of the local surface tension. Due to the distinct structures and mechanisms of those catalytic and stimuli-driven hydrogel motors, here we define them as hydrogel surface swimmers. Similar to their biological counterparts, such as water treaders *Mesovelia* and beetle larvae *Pyrrhalta*,[40] these hydrogel surface swimmers move by the manipulation of the water−air interface. The Marangoni effect is the mechanism behind most of the interesting phenomena, as demonstrated by the nonuniform surface tension distribution and liquid flow caused by either thermal gradient[41] or additional surfactant.[42] As an addition to the existing mechanisms, recently, our group discovered a water-strider-inspired hydrogel robot that is capable of fully autonomous movement on the water surface. This novel robotic system does not require additional surfactant nor operated stimuli to generate locomotion, and it is driven by a new mechanism called dynamic wetting.[43]

Despite the progress made in expanding both the mechanism and functionality of hydrogel robots, it is still a challenge to tackle complex tasks in dynamic environments, which sometimes even impose contradictory requirements on the properties of the robot. Taking biomedical applications as one example in order to accomplish biological operations *in vivo*, the softness of the robot body to guarantee the adaptability to pass through narrow channels such as lymphangion or capillary vessels is required, but on the other hand, the mechanical strength of a soft robot to penetrate blood clots or release drugs in deep tissues is required.[44,45] Currently, the intrinsic softness and mechanical hysteresis of polymer networks, the time-consuming swelling process, and low energy conversion efficiency are the limiting factors that restrain the energy density and power output of the hydrogel robotic systems. Notably, the recent advances made in new materials and biomimetic actuation strategies have helped to overcome the limits in exerting large deformation, high actuation frequency, and large forces in hydrogel robots. Further, the ability to perform complex shape morphing and to respond to multiple physical fields has been proven to be critical to increase the degree of freedom in locomotion and enrich the robot's dynamic interaction with its surroundings.

This perspective aims to provide a panoramic discussion of the design, function, programmability, and intelligence of hydrogel robots. First, we give a comprehensive introduction to existing hydrogel robotic systems and classify them according to their structure and driving mechanisms. Then, we highlight the recent progress made in expanding the mechanism and functionality and improving the performance of hydrogel robots and motors. Finally, we discuss the advances made in bioinspired

https://doi.org/10.1021/acs.chemmater.2c01960
Chem. Mater. 2022, 34, 9307−9328

structures and mechanisms that allow hydrogel robots to exceed current engineering practices and enable them to perform agility, maneuverability, and dexterity that are comparable to natural organisms. With the understanding of the progress and trends in existing hydrogel robots, we propose reasonable directions for the design of future hydrogel robotic systems with high efficiency, robustness, intelligence, and programmability.

2. HYDROGEL SENSORS IN RESPONSE TO COMPLEX ENVIRONMENTS

The sensor is a constituent element of machines that perceives and responds to signals in the environment. While biological nervous systems are soft, water-containing fibers that comply with the motion of the musculoskeletal system, the existing electronic sensing devices are mostly built with materials with high modulus and zero water content, such as semiconductors and metallic electrodes.[46] For typical soft robots, the achievement of self-regulated actuation with closed-loop feedbacks requires mounting sensing elements that are sufficiently compliant, rather than confining the properties or causing stress concentrations of the whole soft structure. However, the current stiff electronic integrations restrict the miniaturization and higher-level motility of the devices.[47] Hydrogels with their excellent combination of softness, conductivity, biocompatibility, and versatility in electrical engineering have become a popular choice for electrodes in soft biocompatible sensing devices.

Hydrogel sensors can actively exhibit volumetric or phase changes upon sensing environmental inputs ranging from temperature[48,49] to humidity,[50] chemicals,[9] and electric fields[51] or passively respond to magnetic fields,[52] pressure,[53] human motion,[54] or biomolecules[19,55] by being incorporated with active substances (such as magnetic particles, conductive polymers, carbon nanotubes, etc.) within the hydrogel matrix. Driven by diverse mechanisms, hydrogel sensors are capable of exerting outputs in the form of mechanical,[52] optical,[50] and electrical[54] responses. The synthesis of soft, conductive, biocompatible, and biodegradable hydrogel sensors potentially provides a seamless interface between biology and the device. Here, we introduce the principle and mechanism of stimuli-responsive hydrogels and hydrogel sensors and give examples of their applications in various fields.

2.1. Stimuli-Responsive Properties of Hydrogels and Their Composites.

2.1.1. Thermally Responsive Hydrogels. Temperature changes in the environment are one of the most prominent stimuli that control the biological rhythm on our planet. Thus, thermally responsive actuation systems are of significant importance for both scientific and industrial applications. The development in polymer chemistry has allowed synthetic hydrogels to undergo significant volume transition under temperature changes.[27,56] Thermally responsive hydrogels usually show a lower critical solution temperature (LCST) or an upper critical solution temperature (UCST). The LCST transformation process involves breakage and formation of hydrogen bonds with water molecules.[57] Above the LCST, the hydrogen-bending interactions are decreased and thus the hydrogels are in a collapsed, shrunken state. A temperature-driven actuation system in the range compatible with the human body is critical for biomedical applications. One of the most popular temperature-responsive hydrogel systems is poly(*N*-isopropylacrylamide) (pNIPAm) and its derivatives, because it exhibits large volume changes at a relatively low LCST temperature of around 32 °C.[27] With an increase in temperature across the LCST of pNIPAm, a coil to globule transition occurs, which causes the hydrogel to shrink and become opaque. The LCST can be tuned by varying the molecular weight, polarity, functional group, and copolymerization.[58]

The UCST transformation process involves the association and disassociation of H-donors and H-acceptors to polymer chains.[48] In contrast to LCST hydrogels, the UCST-type transition leads to the expansion or swelling of hydrogels above the critical temperature. When poly(acrylic acid) (pAAc) and poly(acrylamide) (pAAm) are copolymerized into an interpenetrating hydrogel, a UCST-type transition is exhibited. Researchers have made efforts to create hydrogels showing both the LCST and UCST; one example of a clay/p(MEO_2MA-*co*-OEGMA) nanocomposite hydrogel was fabricated by polymerization of 2-(2-methoxyethoxy) ethyl methacrylate (MEO_2MA) and oligo(ethylene glycol) methacrylate (OEGMA) in an aqueous solution with cross-linker clay. The obtained nanocomposite hydrogels exhibited double volume phase transition behaviors, corresponding to the LCST and UCST, with reversible thermosensitivity.[59]

2.1.2. Optically Responsive Hydrogels. Light is a clean, safe, and sustainable energy source that can be easily and precisely tuned in terms of its intensity, polarization, wavelength, and repetition frequency. The application of light to manipulate small-scale objects can be classified into three main mechanisms: photophoretic effects,[60] photochemical effects,[23] and photothermal effects.[41] Optical trapping based on the photophoretic effect permits a fine and precise control of the colloidal particles suspended in air or liquid, but it usually generates a force on the order of picoNewtons (10^{-12} N), which limits the size of objects that can be lifted. Photochemical hydrogels are functionalized by physical or chemical cross-linking with specific photoresponsive chemical materials such as azobenzene, spiropyran, nitrobenzene, or cinnamoyl groups, which changes their molecular properties such as configuration, cross-linking degree, and photolysis under the light stimulus.[17] The photoactive molecule azobenzene absorbs light and undergoes a *cis* to *trans* configuration transformation, which causes reversible geometrical changes under light irradiation at specific wavelengths, and another well-studied photochromic chemical, spiropyrans, undergoes an electrocyclic ring-opening reaction from a closed spiro form to a planar merocyanine form upon ultraviolet (UV) light illumination.[61] Although photochemically active hydrogels show geometric programmability upon light irradiation, this method usually suffers from a relatively small deformation.

Although hydrogels have limited photothermal efficiency, the embedment of other photothermal substances such as carbon-based nanomaterials, metallic nanoparticles, two-dimensional (2D) semiconductors, and transition metal sulfides can bring about significant improvement in the photothermal efficiency. Carbon-based nanomaterials, such as reduced graphene oxide (rGO)[24,33] and carbon nanotubes (CNTs),[62] are excellent photothermal agents due to their superior photothermal conversion efficiency. The high strength of carbon nanomaterials also enables the enhancement of the mechanical properties and swelling ratios of the hydrogels when dispersed in the polymer matrix[63,64] or used as three-dimensional building blocks.[65] The localized surface plasmon resonance (LSPR) effect that occurs in nanosized metallic particles is the main mechanism that makes metallic particles such as gold nanoparticles (AuNPs),[22,66] Fe_3O_4 nanorods,[21,67] and copper nanoparticles (CuNPs)[68] prominent photothermal agents. The photothermal heating occurring in the near-infrared

https://doi.org/10.1021/acs.chemmater.2c01960
Chem. Mater. 2022, 34, 9307−9328

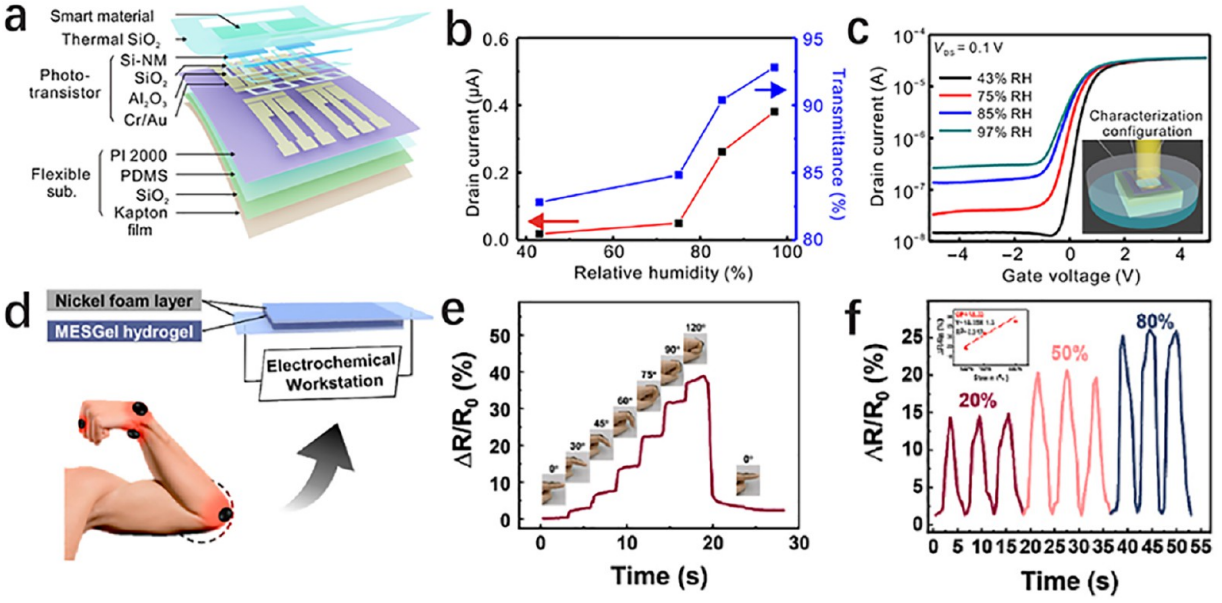

Figure 2. Typical hydrogel sensors. (a) Schematic illustration of a flexible sensor with a semiconductor phototransistor covered by stimuli-responsive hydrogel layers. (b) Variation trend of the output signal and transmittance of the hydrogel film with the increase of relative humidity. (c) Transfer curves of the device at various relative humidities under gate voltage changes. Reproduced with permission.[50] Copyright 2020, AAAS. (d) Schematic illustration of a hydrogel sensor toward monitoring human joint movement. (e) Bending angle detection of a finger. (f) Relative resistance changes under compressive strains. Reproduced with permission.[54] Copyright 2021, Elsevier.

(NIR) range has great potential for biomedical treatment with its considerable penetration depth, low phototoxicity, and high space−time remote control ability.[33] Novel 2D functional materials with high specific surface areas provide remarkable NIR absorption capacity and abundant anchoring sites to load therapeutic agents. The MXene nanosheets with unique 2D nanostructures exhibit excellent photothermal effects and thermal conductivity, leading to a localized temperature change under NIR irradiation.[69]

Recently, nonlayered MoO_2 nanosheets have been studied in terms of their LSPR mechanism, NIR absorption efficiency, chemical stability, and toxicity. The synthesized hydrogel/MoO_2 composites have shown potential for applications in photothermal actuators and microfluidic devices.[70] Different from the above photochemical or photothermal agents that absorb light within a narrow range of wavelength, it would be ideal if novel photoresponsive materials exhibited broadband light absorption from the UV−visible to infrared region. Such advanced materials could be constructed by rationally designing the porous structure, hierarchical networks, and nanowire alignments of the known material libraries.[23,71]

2.1.3. Magnetically Responsive Hydrogels. Magnetic fields provide untethered control over the spatiotemporal deformation of magnetic soft materials. The biocompatibility and penetrability of the magnetic field to most biomaterials and inorganic materials enable remote manipulation of objects in isolated and confined environments.[72] Basically, hydrogels embedded with ferromagnetic particles can receive magnetic torque or magnetic force from the external magnetic fields. The magnetic torque, provided by a uniform magnetic field generated by one or several pairs of Helmholtz coils, is often used for the precise control of the deformation and locomotion of magnetic soft robots.[72] With the ferromagnetic particles such as Fe_2O_3 or nickel nanorods aligned within the hydrogel in a predesigned direction, it creates a magnetic shape anisotropy that makes the aligned direction the easy axis for magnetization. When the magnetic torque rotates the magnetization away from equilibrium, the magnetically anisotropic material tends to align its magnetization with its easy axis.[72] Thus, the continuously distributed magnetization within the soft hydrogel can produce locally varying stress when it interacts with the magnetic fields.[73] Moreover, when the applied field strength exceeds the coercivity of the magnetic particles, it reprograms the magnetization direction toward the field. These unique features of magnetic composites provide a feasible way to endow the programmability of the hydrogel materials, making it possible to generate complex deformation and morphology under magnetic fields.[29,74,75]

On the other hand, the magnetic force arises from the magnetic field gradient, which is usually generated by a permanent magnet.[31] While the magnetic force could directly pull a magnetic robot toward the desired direction, this method suffers from the significant damping of the magnetic field strength with the increasing distance from the magnet. In addition to the above-mentioned two strategies, magnetic heating utilizes the joule heat generated by the alternating current (AC) magnetic field. In this case, magnetic particles act as heating sites that control the temperature-dependent swelling behavior of the hydrogel or melt specific components to achieve predesigned functions, such as the release of drugs.[76]

2.1.4. Chemically Responsive Hydrogels. By mimicking the natural organisms' dynamic response to the sensing of chemical molecules from the environment, chemical responsive hydrogels offer opportunities for the development of smart and adaptive actuation systems. Chemical reactions with hydrogels are diverse because of the difference in the chemical synthesis of different hydrogels, which enable complex swelling behaviors and changes in optic, mechanical, or electric properties.

Typical chemical responsive hydrogel materials involve the Belousov−Zhabotinsky (BZ) reaction in which the organic substrate experiences a periodic redox reaction in the presence

https://doi.org/10.1021/acs.chemmater.2c01960
Chem. Mater. 2022, 34, 9307−9328

of a metal ion catalyst. The BZ catalyst ruthenium(II) tris(2,2′-bipyridine) ($[Ru(bpy)_3]^{2+}$) could be covalently bonded to the polymer chain of a pNIPAm hydrogel, which results in a self-oscillatory swelling and deswelling process following the nonlinear BZ reaction.[35] Another chemical responsive mechanism of active hydrogel materials includes the oxidation of glucose. The oxidation of glucose to gluconic acid by the enzyme results in a drop in the pH, which can trigger volumetric transitions in a pH-responsive hydrogel matrix.[9] The ionic strength in aqueous solution also leads to a volumetric change of the hydrogel. The pNIPAm undergoes a dehydration process when immerged into a NaCl solution.[28] Also, novel silk−elastin-like protein (SELP) hydrogels exhibited high deswelling ratios in a NaCl solution.[56]

2.1.5. Other Responsive Hydrogels. Hydrogel materials with different chemical structures of the polymer chain or additive in the polymer network result in diverse stimuli-responsive properties. Except for the typical thermal, optic, magnetic, and chemical responsive materials mentioned above, we give a brief introduction to other types of stimuli-responsive hydrogels here. In response to the electric field, the directional migration and rearrangement of ions inside the hydrogel create an osmotic pressure that drives the hydrogel's swelling or deswelling process.[77] The main advantage of this approach is that it allows accurate voltage/current control with commercial software and electric devices, but on the other hand, the electric pulses are not safe for biological tissues when exceeding a certain magnitude.

The pH-responsive hydrogel holds potential in biomedical applications because the pH value varies widely in different organs of the human body and is associated with health conditions and many diseases.[78] The pH-responsive properties mainly arise from the ionizable pendant groups on the polymer backbone, which result in a charge buildup along with the polymer when exposed to a specific pH strength. With the oppositely charged ions penetrating the hydrogel, it causes an increase in osmotic pressure that drives the volumetric change of the pH-responsive hydrogels.

2.2. Application of Stimuli-Responsive Hydrogels toward Integrated Sensors. The stimuli-responsive performance and compatibility of soft hydrogel materials make them suitable for the cooperation of existing sensing and robotic systems. The different mechanisms and performances from conventional bulky electronics have brought new light toward the flexible, integrated, and biocompatible applications. To realize these advances, the combination of different functional ultrathin components with a wafer-compatible process is one of the central tasks. Li et al.[50] demonstrated a flexible optoelectronic humidity sensing system with the humidity-responsive hydrogel layers coated above a flexible silicon nanomembrane phototransistor. A UV-cured hydroxyethyl methacrylate−acrylic acid copolymer hydrogel film of ∼20 μm thickness was chosen as the smart sensitive material and stuck on the top surface of the light-sensitive area (Figure 2a). Upon a humidity change in the environment, the hydrogel film's transmittance increased with an increase in humidity, and the resultant output current of the phototransistor increased in a similar trend (Figure 2b). With the rising of gate voltage, the output current exhibits an abrupt linear increase at a certain inflection point, providing guidance for the optimization of the working conditions (Figure 2c). Such on-chip humidity sensing based on stimuli-responsive hydrogel films benefits the miniaturization of devices and the seamless integration of smart sensing materials with Si CMOS-compatible flexible phototransistors.

Despite the active hydrogel sensors that exploit the intrinsic stimuli-responsive properties of hydrogels, the incorporation of active substances (such as carbon materials, metallic nanoparticles, living cells) into biocompatible hydrogels has provided a unique opportunity to enrich their sensing properties toward biological applications.[79] Zheng et al.[54] employed an integrative cross-linking strategy to combine conductive poly(3,4-ethylenedioxythiophene):polystyrenesulfonate and multiwall carbon nanotubes into a gelatin-based biocompatible hydrogel. The conductivity and mechanical properties of the hydrogel composite increased with the addition of dispersion phases and thus rendered it electroactive and responsive to human joint motions at the knuckle, elbow, and wrist (Figure 2d), as demonstrated by the change in the relative resistance ($\Delta R/R_0 \times 100\%$) of the hydrogel composite sensor. They found that the $\Delta R/R_0$ increased with the increase of the bending degree at different joints at a short response time of 100 ms (Figure 2e). Their hydrogel composite sensor could also respond to compressive strains (Figure 2f), indicating the potential of the conductive hydrogel composites as epidermal sensors.[54]

The low modulus and high electrical conductivity are the key requirements of hydrogel sensing devices. Ye et al.[80] combined CNTs with pAAm to form a cathode and anode of a hydrogel battery. It was found that, after full dehydration and partial rehydration, the electrical conductivity of the hydrogel electrodes was significantly improved from 0.8 to 1×10^3 mS cm^{-1}, which was attributed to the reduced interface resistance of the electron transport of CNTs and reduced pore sizes in the hydrogel network. A similar strategy was adopted to form a high-conductivity hydrogel composed of partially dehydrated pAAm−alginate embedded with a low concentration of Ag flakes.[81] The resulted hydrogel composite exhibited a high electrical conductivity of >350 mS cm^{-1} and Young's modulus of <10 kPa, which allowed it to sense the applied strains and to be integrated into diverse robotic and healthcare devices. In addition, thermal regulation is important for the stable function of robotic devices in autonomous operations. Mishra et al.[82] utilized the responsive properties of micropores (∼200 μm) made by pAAm capped on a 3D printed fluidic elastomer actuator, which endowed it autonomous thermal regulation capability (∼107 W kg^{-1}) by perspiring through the microporous surface. Such a strategy offers an entirely passive way for autonomous thermal regulation of future soft robotic devices.

Microbial sensing is an attractive diagnostic application through the detection of disease-associated biomolecules within the human body. Liu et al.[52] developed a magnetic living hydrogel system consisting of an ingestible poly(vinyl alcohol) (PVA) hydrogel composite loaded with NdFeB magnetic particles and diagnostic microbes. Different from traditional retaining devices that are prone to intestinal blockage or device migration, the magnetic particle within the hydrogel facilitated localization and was retained in the gastrointestinal tract. Due to the softness of the hydrogel, the diagnostic device is geometrically compliant to the inner wall of the gastrointestinal tract, thus avoiding intestinal blockage problems and minimizing tissue damage. The living biosensing bacteria integrated into the soft hydrogel matrix were retained in vitro for 7 days and could detect bleeding in a mouse intestine.[52] Other examples of hydrogel sensors for typical applications such as protein detection, photosensor measurements, and sweat detection are found in the literature.[55,83,84]

https://doi.org/10.1021/acs.chemmater.2c01960
Chem. Mater. 2022, 34, 9307−9328

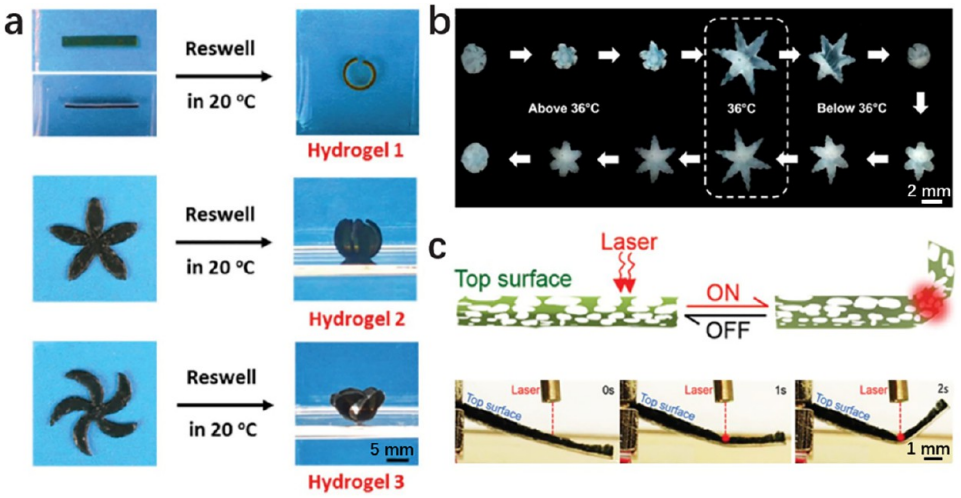

Figure 3. Hydrogel actuators with layered or gradient structures. (a) Bilayer PBI-HPEI/GO-pNIPAm hydrogel actuators bend and form folded structures upon temperature changes. Reproduced with permission.[78] Copyright 2018, Wiley-VCH. (b) Reversible thermal actuated self-folding of a layered hydrogel actuator placed in deionized water. Reproduced.[92] Copyright 2015, American Chemical Society. (c) Laser-induced bending deformation of a hydrogel strip with a gradient porous structure. Reproduced with permission.[91] Copyright 2015, Wiley-VCH.

3. HYDROGEL SOFT ROBOTS ACTUATED BY OSMOTIC-DRIVEN DEFORMATION

Smart deformations in nature are characterized by the generation of a time-dependent deformation profile along a living organism's soft body in a dynamic interaction with the environment. With the deepened understanding of the motion behaviors of biomimetic structures, awareness has been raised that the continuum deformation of soft robots would be the key to the miniaturization of robotic devices and that artificial machines could successfully mimic the agile shape morphing, functionality, and gaits of their natural counterparts.[85] The construction of soft robots with stimuli-responsive active materials is a prominent approach to integrate different energy conversion mechanisms inside a soft body, and the combination of a specific structure design allows them to generate desired time-varying shapes and programmable locomotion models.[16] The development of materials science and mechanical engineering has stimulated advances in both aspects and pushed hydrogel soft robots toward novel functionalities.[86] In this section, we introduce the principle in the design of deformation-actuated hydrogel soft robots and highlight the progress made in improving the actuation efficiency, high degree of freedom in locomotion, and novel functionalities.

The anisotropic and patterned structures are key to achieve diverse functions of smart actuation systems.[87] As a homogeneous and unstructured hydrogel only undergoes an isotropic volume change through swelling and deswelling processes, the structure design and patterning of hydrogels enable complex shape changes and thus various functions in response to different stimuli.[21,88] We classify and discuss different deformation structures and mechanisms below.

3.1. Anisotropic Structures of Hydrogel Soft Robots.

3.1.1. Hydrogels with Layered and Gradient Structures. A classic layered structure is composed of hydrogel layers with different moduli or swelling behaviors, which leads to an anisotropic volumetric change and the buildup of internal stresses. Usually, fabrication methods such as multistep molding, spin coating, or lithography are used to combine different layers and control their thickness. Upon applying stimuli, such as temperature changes, the layer utilizes the strain gradient generated by the different swelling behaviors and mechanical properties of the individual layers to create out-of-plane bending or folding deformations.[86]

The bending deformation of a bilayer hydrogel actuator under homogeneous field actuation can be predicted by the Timoshenko beam theory,[2,89] where the bilayer with a large difference in the coefficient of expansion, mechanical strength, and geometry parameters could generate considerable bending deformation. Stoychev et al.[90] investigated the folding behavior of hydrogel bilayers with different aspect ratios and thicknesses. They found that long-side rolling dominates at high aspect ratios and rolling from all sides occurred when the width and length considerably exceed the circumference of a deformed state. The variety of rolling scenarios could be ascribed to the non-homogeneous swelling and the adhesion of the hydrogel layer to the substrate.[90] Ma et al.[78] combined a thermally active graphene oxide-poly(*N*-isopropylacrylamide) (GO-pNIPAm) hydrogel layer with a pH-responsive fluorescence perylene bisimide-functionalized hyperbranched polyethylenimine (PBI-HPEI) layer to form an anisotropic bilayer structure that bends upon a temperature change. By cutting the bilayer sheets into different shapes, they obtained different temperature-triggered 3D shape morphing models (Figure 3a). Breger et al.[92] combined poly(*N*-isopropylacrylamide-*co*-acrylic acid) (pNIPAm-AAc) with stiff nonswelled polypropylene fumarate (pPF) layers to fabricate microgrippers that exhibited reversible actuation upon a temperature cycle (Figure 3b). The combination of the swelling layer with a passive layer could only result in unidirectional bending; it is therefore reasonable to employ layers with distinct swelling behaviors to achieve more complex bidirectional deformations. Li et al.[57] synthesized a bilayer hydrogel actuator that consists of a UCST-type poly(*N*-acryloyl glycinamide) (pNAGA) layer with a LCST-type poly(*N*-isopropylacrylamide) (pNIPAm)−Laponite nanocomposite layer. The complementary swelling behaviors of the UCST- and LCST-type hydrogels give the actuator a fast bending ability and bidirectional bending behavior when across the UCST and LCST transition.

Compared to layered structures that have mismatch problems between the combined materials, the seamless gradient structure

https://doi.org/10.1021/acs.chemmater.2c01960
Chem. Mater. 2022, 34, 9307−9328

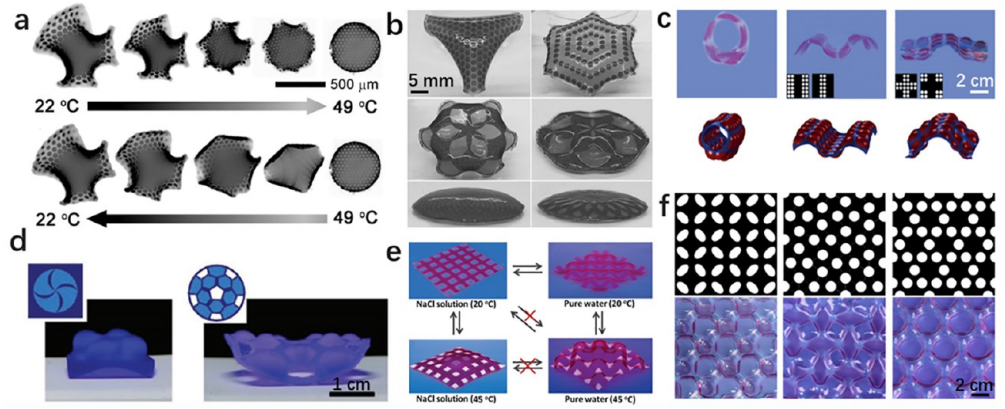

Figure 4. Hydrogel actuators with patterned structures. (a) Thermal actuation of patterned hydrogel discs consisting of high swelling and low swelling regions. Reproduced with permission.[93] Copyright 2012, AAAS. (b) 3D shape changes of surface patterned hydrogels. Reproduced with permission.[94] Copyright 2017, Wiley-VCH. (c) Preswelling-directed shape morphing of patterned hydrogel sheets. Reproduced with permission.[95] Copyright 2017, Wiley-VCH. (d) Out-of-plane deformation of a hydrogel printed with a selected exposure time at different positions. Reproduced with permission.[88] Copyright 2017, Wiley-VCH. (e) Reversible step-by-step deformations of a multilevel structure. Reproduced with permission.[96] Copyright 2019, Wiley-VCH. (f) Deformation of periodically patterned hydrogels showing cooperative deformation of the neighboring units. Reproduced with permission.[97] Copyright 2017, AAAS.

is beneficial for avoiding stress concentrated at the interface. Utilizing gradient distribution of the dispersion phase, such as pores, precipitates, or additional particles, would effectively generate an anisotropic strain distribution and dissipate excessive stress to the whole structure, such that the damage caused by stress localized at the interfaces could be avoided. Luo et al.[91] used *N*-isopropylacrylamide as monomers to polymerize with 4-hydroxybutyl acrylate (4HBA) via a hydrothermal reaction, during which the precipitation of pNIPAm−OH hydroxyl groups leads to a concentration gradient from the top to bottom of the hydrothermal reactor. The resulted gradient porous hydrogel strip can bend upon a uniform temperature increase or localized laser irradiation (Figure 3c).

3.1.2. Hydrogels with Patterned Structures. As the anisotropic layered and gradient structures make it easy to form bending deformations, the controlled buckling of planar sheets is the pathway to form complex 3D shapes. Spatially nonuniform swelling developed by stimuli-responsive hydrogels with patterns of varied sizes and geometric arrangements is an attractive approach to induce such complex out-of-plane shape morphing. Kim et al.[93] employed a half-tone lithography process to pattern pNIPAm hydrogel sheets containing pendent benzophenone units, which allows tunable cross-linking at specific sites by controlled irradiation doses. The patterned architecture consisted of highly cross-linked dots embedded within a lightly cross-linked matrix, and the stress distribution generated by nonuniform swelling enabled smart transformations of flat sheets into spherical caps, saddles, cones, and Enneper's surfaces (Figure 4a). Peng et al.[94] developed an ion inkjet printing technique that allows for the batch fabrication of complex patterns with programmable cross-linking densities. The printing process was completed in a ferric solution where the complexation between polyelectrolyte and ferric ions increased the cross-linking density of the patterned dots. The adjustment of printing times and grayscale distributions of patterns resulted in the formation of different 3D shapes (Figure 4b).

The stress gradient distributed along the thickness direction of the layered and gradient structures can effectively determine the bending direction, but in patterned structures, the in-plane gradient-induced buckling deformation usually has self-locked bistable states, which makes the direction of buckling unpredictable. In order to address this unpredictability, Zheng and co-workers[95] employed a preswelling step to embed a transient through-thickness gradient of patterned high swelling regions, so that the buckling of individual domains could be directed, forming programmable configurations in the following swelling step (Figure 4c). As the photolithography approach is used for patterning in most cases, it lacks the capability to generate high resolution and time-varying patterns. Huang et al.[88] demonstrated a printing setup that consists of a computer-controlled projector embedded with a digital micromirror device (DMD) and a reaction cell containing light-curable monomers. This setup is capable of millisecond-scale control of the light exposure so that a pixelated sample can be printed at a very fast speed and turn into 3D objects when immersed in water (Figure 4d).

Another approach to pattern advanced hydrogel actuators is the integration of different responsive materials to form a multilevel structure. On the basis of this concept, Ma et al. sequentially patterned pAAm, pNIPAm, and poly(acrylamide-*co*-2-acrylamido-2-methylpropanesulfonic acid) [p(AAm-*co*-AMPS)] gels in multistep photolithography to form periodic arrangements. The hydrogels with distinct swelling properties at specific sites were able to reversibly transform into 3D configurations on the basis of the change in ion strength and temperature (Figure 4e).[96] When the deformed units were close to each other in a patterned structure, the interaction and cooperation of neighboring units determined the overall shape change of the structure. Wang et al.[97] demonstrated the cooperative deformation of 2D periodically patterned hydrogel sheets with alternating geometry and gel properties. While the high-swelling regions buckled to relieve the in-plane compressing caused by the constraining effect of nonswelling regions, the whole structure remained flat due to the cooperative deformation of the neighboring units (Figure 4f).

3.1.3. Hydrogels with Oriented Structures. The differential distribution of the fiber orientations among plant cells can collectively generate anisotropic movements in the overall plant tissue[98] and transforms the osmotic pressurization and hygroscopic swelling into bending, twisting, and buckling deformations.[99,100] Such effects of oriented cellulose fibril on

https://doi.org/10.1021/acs.chemmater.2c01960
Chem. Mater. 2022, 34, 9307−9328

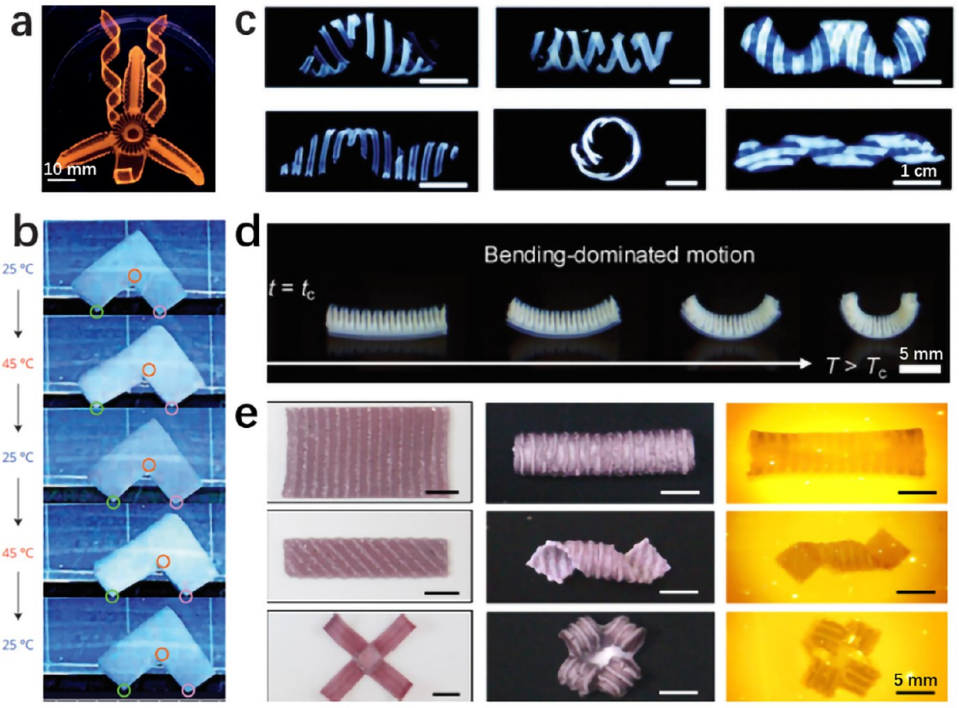

Figure 5. Hydrogel actuators with oriented networks. (a) Complex flower morphologies generated by biomimetic 4D printing. Reproduced with permission.[101] Copyright 2016, Nature Publishing Group. (b) Unidirectional procession of an L-shaped symmetric TiNSs/pNIPAm hydrogel actuator. Reproduced with permission.[102] Copyright 2015, Nature Publishing Group. (c) Shape transformation of a composite hydrogel sheet into a left-handed helix, rolls, and a right-handed helix. All scale bars are 1 cm. Reproduced with permission.[103] Copyright 2016, The Royal Society of Chemistry. (d) Orthogonally oriented bilayer network structures with a saddle-like shape change and bending motion. Reproduced with permission.[104] Copyright 2019, Wiley-VCH. (e) Various shape changes of hydrogel networks containing oriented AuNPs induced by a photothermal effect. All scale bars are 5 mm.Reproduced with permission.[22] Copyright 2020, Nature Publishing Group.

plant movements have inspired many biomimetic structures and actuators. In order to encode the anisotropic mechanical response of the hydrogels, the construction of elaborate heterogeneous network structures to tune the mismatch and internal stress of individual components is the central issue.

Sydney Gladman et al.[101] printed composite hydrogel architectures with the alignment of cellulose fibrils along redesigned pathways. The localized and anisotropic swelling behavior is programmed by the fibril distribution, allowing plant-inspired smart structures to perform complex 3D shape morphing when immersed in water (Figure 5a). Kim et al.[102] adapted oriented lamellar electrolyte titanate nanosheets (TiNSs) inside a pNIPAm hydrogel. The specific arrangement imparts a large anisotropic electrostatic repulsion inside the hydrogel matrix. Upon the LCST transition, the internal electrostatic permittivity of pNIPAm changed reversibly and the distance between the TiNSs rapidly expanded and contracted on heating and cooling. The resulted thermal-induced large shape change occurred without substantial water uptake and release. As a demonstration of the oriented TiNSs/pNIPAm actuator, a L-shaped bipedal walking hydrogel was able to proceed unidirectionally upon a temperature change (Figure 5b).

Wang et al.[103] fabricated layered fibrous structures that mimic a bean pod with programmed deformations. The responsive structure contains cellulose fibrils of pAAc/pNIPAm and pNIPAm as interpenetrating networks with different swelling ratios and moduli. When switched between pH = 9 and pH = 1, the destruction and recovery of the hydrogen bonds between the amide groups of pNIPAm and the carboxyl groups of pAAc produce orthogonally distributed internal stress that drives the transformation of the planar structure into a twisted helix, and when the geometry parameters of the individual layers were tuned, other forms of the deformed structure such as a cylindrical helix and rolls could be obtained (Figure 5c). Similarly, Arslan et al.[104] printed orthogonally arranged poly(ethylene glycol) (PEG) reinforcement elements in a pNIPAm matrix to induce anisotropic actuation of the individual layers, and the resulted bilayer structures were able to perform bending and twisting deformation upon temperature modulation (Figure 5d).

Zhu et al.[22] employed multistep electrical orientation and photolithography to align $[Na_{0.5}][Li_{0.5}Mg_{2.5}][Si_4]O_{10}F_2$ nanosheets within a hydrogel precursor containing AuNPs. They used a high-frequency AC electric field to orient the nanosheets, such that nanosheets with a large aspect ratio act as stiffeners against in-plane deformation, making the modulus along the parallel direction much larger than that of the vertical direction. The combination of AC electric field orientation and multistep photolithography enabled the construction of domain structures with periodic orientations, so that upon photothermal actuation the deformation mismatch between neighboring domains would result in the buildup of internal stresses. The hydrogels with different domain orientations and arrangements were encoded with various 3D deformation patterns, which resulted in the formation of tubes or left- or right-handed helices upon a temperature increase (Figure 5e).

3.2. Locomotion of Hydrogel Soft Robots by Deformation. Hydrogels have broad applications in the field of soft robots due to their softness, biocompatibility, and stimuli-

https://doi.org/10.1021/acs.chemmater.2c01960
Chem. Mater. 2022, 34, 9307−9328

Table 1. Comparison of the Different Structures, Mechanisms, and Applications of the Deformation-Driven Hydrogel Robots

structure	deformation type	mechanisms	fabrication method	bending angle (deg)	size (mm)	stimuli	function	ref
layered structure	bending	strain gradient generated by different layers	photolithography	60	6	temperature; magnetic field	gripping	92
	bending	strain gradient generated by different layers	molding	75−82	22	temperature	gripping	57, 78
	bending	strain gradient generated by different layers	molding	46	34	temperature	crawling	111
	oscillation	continuous steam generation	molding	40	35	light	swimming	21
gradient structure	bending	strain generated by gradient porous structures	molding	90	20	light; temperature	gripping; swimming	91
patterned structure	bending; twisting	anisotropic swelling programmed by orientation	photolithography	45	10	light	crawling	22
	bending; twisting	anisotropic swelling programmed by oriented multiresponsive network	photolithography	65	18	ion; light; pH; temperature	gripping	112
	bending; twisting	site specific swelling	molding	82		light	gripping	113
strip	bending; twisting	temperature gradient induced by structured light	molding	70	6	light	rolling	23
	bending	temperature gradient induced by structured light	molding	60	9	light	swimming	114
	bending; twisting	magnetic torque exerted by an oscillating magnetic field	molding		4	magnetic field	crawling; rolling; swimming	74
sphere	expansion	bubble generation induced by a photothermal effect	suspension polymerization		2	light	jumping	67
elastic chamber	bending	pneumatic/hydraulic pressure induced inflation	3D printing	90	100	pressure	gripping	105, 115

responsive swelling properties. However, existing hydrogel actuators, mostly osmotic pressure-driven, involve a time-consuming diffusion and rearrangement of water inside the polymer networks.[105] Furthermore, because the polymer networks have characteristic long polymer chains between cross-link points, many hydrogel systems undergo hysteresis during cyclic deformation due to pronounced energy dissipation.[106] In this part, we introduce recent progress made in various applications of hydrogel robots with a special focus on those designs of new materials and actuation mechanisms that help to overcome the intrinsic low speed and force of hydrogel actuation systems. To gain a comprehensive perspective of deformation-driven hydrogel robotic systems, a comparison of the different structures, mechanisms, and applications of hydrogel robots driven by deformation are listed in Table 1.

Gripping is a universal motion by which animals and plants interact with the environment or other objects.[107] While the layered structure utilizes the strain gradient and mismatch to generate bending deformation, it is easy to transform a layered hydrogel into a stimuli-responsive gripper through structure design. Examples of hydrogel grippers can be triggered by temperature,[78] light irradiation,[108] solvent,[109] etc., but the response time of these osmotic-driven actuators ranges from minutes to hours. An alternative approach for fast grasping is to embed inflatable chambers and channels on one side of the hydrogel actuators to directionally deform the structure. Such structures are usually made of silicone elastomer components and are challenging for hydrogels because of the insufficient robustness and stiffness. To overcome this drawback, Yuk et al.[105] fabricated pAAm-alginate tough hydrogels with a fluidic chamber structure that utilize hydraulic actuation instead of osmotic pressure to achieve fast grasping of a living goldfish (Figure 6a). This approach allowed the actuators to exert a force larger than 1 N with a response time of less than 1 s. A detailed comparison of the actuation force and frequency of different hydrogel actuators is given in Table 2.

Besides gripping, other basic locomotion modes such as rolling, crawling, and walking are adapted by animals to avoid predators and to access enclosed and confined environments. As the transformation of hydrogels is related to the water release and uptake process, much effort has been made to realize complex underwater deformation and movement. While most underwater hydrogel actuators are temperature-driven, the environmental temperature, which is too slow for fast switching, needs to change.[57,78] On the other hand, light-driven photochemical or photothermal transitions are much faster and enable programmable local actuation by changing the spot shape, irradiation position, frequency, or strength.[21−23] Xiang et al.[23] constructed polyurethane (PU) hydrogels containing dual networks of dynamic covalently cross-linked hexaarylbiimidazole (HABI) units. Upon light irradiation, the cleavage of the C−N bond in the photochromic HABI unit caused the decrease in the cross-link density of the hydrogels. Much different from layered or gradient structures, the PU hydrogel strip is homogeneous, but the excellent absorption rate of visible light by the hydrogel resulted in preferential absorption of incident light on the phototropic face and thus anisotropic deformations. Such photochemical transformations allow bending, twisting, and folding deformations upon localized and structured light irradiation. When a rectangular 0.4 mm thick PU hydrogel strip was joined end-to-end to form a wheel, the light irradiation on one side of the wheel shifted its weight center and resulted in phototaxis rolling locomotion under water (Figure 6b).[23]

https://doi.org/10.1021/acs.chemmater.2c01960
Chem. Mater. 2022, 34, 9307−9328

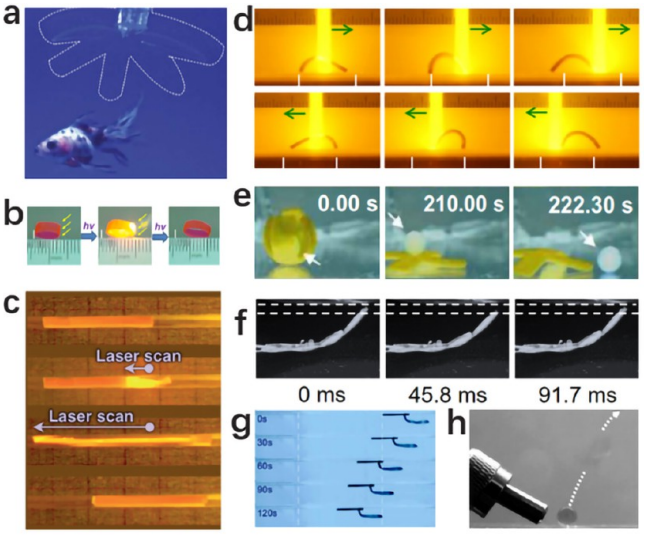

Figure 6. Hydrogel robots with diverse mechanisms, designs, and applications. (a) A transparent hydraulic hydrogel gripper catches a live goldfish. Reproduced with permission.[105] Copyright 2017, Nature Publishing Group. (b) Photochemical-driven forward rolling of a hydrogel actuator under water. Reproduced with permission.[23] Copyright 2021, Elsevier. (c) A cylindrical hydrogel crawling inside a capillary under scanning laser light. Reproduced with permission.[110] Copyright 2018, Wiley-VCH. (d) Bidirectional walking of strip-patterned anisotropic hydrogel under scanning light. Reproduced with permission.[22] Copyright 2020, Nature Publishing Group. (e) Light and magnetic field induced cargo transport and release of a cross-shaped hydrogel film containing aligned Ni nanowires. Reproduced with permission.[29] Copyright 2020, AAAS. (f) Photothermal oscillators powered by local steam generation. Reproduced with permission.[21] Copyright 2021, AAAS. (g) An oscillating swimming hydrogel robot under directional visible light irradiation. Reproduced with permission.[130] Copyright 2019, AAAS. (h) Jumping of a hydrogel sphere driven by photothermal-induced bubble generation. Reproduced with permission.[67] Copyright 2020, Nature Publishing Group.

Limbless creatures in nature often live in narrow and hard-to-access spaces, and they move by sequential expansion and contraction of their body segments. Inspired by the peristaltic crawling of earthworms, Sun et al.[110] demonstrated a hydrogel actuator that enables repeatable and bidirectional crawling inside a capillary. They employed a superstrong magnetic field to align TiNSs within the pNIPAm hydrogel actuator and incorporated them with AuNPs for photothermal energy conversion. Similar to their work in 2015,[102] the photothermal heating switched the electrical permittivity of the polymer network and thus synchronously changed the electrostatic repulsion between the TiNSs. When utilizing light scanning along the hydrogel body, a spatiotemporal deformation profile of elongation and contraction can be generated, which enables earthworm-like peristaltic crawling inside confined spaces (Figure 6c).[110] Zhu et al.[22] adopted a similar structure containing oriented NSs and photothermal receiver AuNPs. Their light-triggered hydrogel actuator achieved bidirectional crawling, walking, and turning using a scanning green light beam along with specific scanning directions (Figure 6d).

Li et al.[29] designed hydrogels by combining a scaffold of high-aspect ratio ferromagnetic nanowires with a polymer matrix containing a photoswitching spiropyran (SP) monomer, which renders the actuator dual-responsive performance upon light irradiation and magnetic field manipulation. The hydrogels rotated by applying a rotating magnetic field due to the magnetic anisotropy of the aligned anisotropic ferromagnetic nanowires, which produced a magnetic torque of $\sim 5 \times 10^{-8}$ Nm. At the same time, they could bend toward the light source because of the creation of a spatial gradient in the amount of hydrophilic and hydrophobic moieties within the hydrogel. The synergistic response allowed fast underwater walking and even delivery of cargo through rolling and subsequent shape changes (Figure 6e).[29] It is notable that the combination of different responsive properties is an advantageous strategy to overcome the limitations of a single type of actuation and to increase the steerability of hydrogel robotic systems; such examples are also found in the combination of ultrasound and temperature,[122] light and ion,[123] temperature and ion,[124] etc.

The energy conversion process of muscles does not involve solvent diffusion and thus endows them with an excellent combination of robustness, high energy density, and high output power.[125] However, on the other hand, traditional osmotic-driven hydrogels require the diffusion of solvents in the polymer network. For osmotic-driven hydrogels, the energy density could be approximated as $\rho_E = \Delta\Pi\varepsilon_s/2$, where $\Delta\Pi$ is the change in osmotic pressure during the swelling process and ε_s is the swelling strain.[126] For some other hydrogel actuators, such as the magnetic-driven or electric-driven ones, they can be regarded as elastomers and the energy density could be approximated as $\rho_E = E(\varepsilon_a)^2/2$, where E is Young's modulus and ε_a is the actuation strain.[85] For power output, the power density $\rho_W = f\rho_E$, where f is the actuation frequency. Although the low modulus of hydrogels is beneficial for deformability and compatibility, it limits the deformation speed and mechanical power output. To overcome these limits on hydrogel actuation systems, new mechanisms must be exploited. Inspired by the oscillation of biological processes such as the heartbeat of mammals, researchers have developed hydrogel oscillation systems on the basis of the

Table 2. Comparison of the Actuation Force and Frequency of Different Stimuli-Responsive Hydrogel Actuators

hydrogel	stimuli	type	actuation force (N)	actuation frequency (Hz)	ref
p(AAc-co-NIPAm)	ion strength	lifting force	0.15		116
PEE-PPy	moisture	lifting force	9.31×10^{-2}	0.33	117
pNIPAm/PVBIPS	temperature	lifting force	2.25×10^{-2}	4.17×10^{-3}	118
PVA/(PVA-MA)-g-pNIPAm	temperature	lifting force	9.8×10^{-3}	3.33×10^{-3}	119
(pAAm)-alginate	pressure	lifting force	1	1	105
pNIPAm	temperature	lifting force	4×10^{-6}		107
pEGDA	acoustic field	propulsive force	9.15×10^{-9}	3.75×10^{3}	120
pAAm/$KMnO_4$	chemicals	propulsive force	1.14×10^{-7}		121
Ca-Alg/pEGDA/IONPs	magnetic field	propulsive force	6.2×10^{-8}	55	45
pAANa/IONPs	light	propulsive force	4.05×10^{-3}		67

https://doi.org/10.1021/acs.chemmater.2c01960
Chem. Mater. 2022, 34, 9307−9328

Table 3. Comparison of the Different Structures, Mechanisms, and Applications of Hydrogel Motors Driven by Chemical Fuels or External Fields

structure	autonomous	fueled	mechanisms	fabrication method	size	stimuli	function	ref
3D printed	yes	yes	bubble recoil induced by catalytic reaction	3D printing	120 μm	magnetic field	swimming	141
Janus particle	yes	yes	bubble recoil induced by catalytic reaction	microfluidic + e-beam evaporation	250 μm	magnetic field	swimming	38
Janus rod	yes	yes	bubble recoil induced by catalytic reaction	cut + coating	6 mm	chemical fuel	swimming	121
core/shell droplet	yes	yes	enzyme-mediated decomposition of fuel	microfluidic lithography	19.8 μm	none	swimming	139
helix	no	no	axial thrust generated by rotation	microfluidic lithography	170−1100 μm	magnetic field	swimming	45, 140
	no	no	axial thrust generated by rotation	template	2.5−3.5 mm	magnetic field	swimming	154, 155
tube	no	no	bubble recoil induced by NIR light	molding	6 mm	light	swimming	39
isotropic disc	yes	no	dynamic wetting	molding	1−4 cm	none	swimming	43

Belousov−Zhabotinsky reaction,[35] nonredox reaction,[127] chemo-mechanochemical self-regulation,[128] and humidity-triggered mechanical oscillation,[129] but these approaches cannot achieve precise untethered control with high degrees of freedom. Instead of the above methods, light actuation can efficiently drive the transition of photochemical or photothermal actuated hydrogels via the embedment of high-efficiency photon receivers.

Li et al.[21] exploited the swimming behavior of a steam-driven oscillating hydrogel actuator under constant stimuli. The key component of the oscillator comprises hydrogels embedded with Fe_3O_4/Cu nanorods that can effectively generate steam bubbles through high-efficient photothermal conversion. Upon light irradiation, the heat generated by nanorods resulted in localized bubble formation followed by bubble collapse, which regularly perturbs the hydrogel film, inducing an oscillation with frequency ranging from 10 to 32 Hz, depending on the light strength (Figure 6f).[21] Similarly, Zhao et al.[130] reported a self-sustained oscillation of highly bendable AuNPs/pNIPAm hydrogels (Figure 6g). The mechanism of the oscillation originated from the self-shadowing effect coupled with the high speed of actuation. When the light-irradiated side of the hydrogel was heated above the LCST, it shrunk and overbent to block further photothermal heating. After cooling to the original temperature below the LCST, the hydrogel returned to its flat shape and was heated again. As compared to other actuation systems in which the mechanical motions are driven by on−off switching of external stimuli, such novel hydrogel oscillators would be promising to realize functions of biological species as they are able to perform regular oscillation under nonperiodic stimuli and alter their oscillating dynamics in response to environmental changes.

Acoustic-driven microswimmers utilize high-frequency oscillation in a more delicate way.[131] Ultrasound is a widely used power source in biomedical applications such as ultrasound imaging, because it is safe for most biological systems and provides noninvasive penetration in deep tissues.[132,133] The acoustic-driven hydrogel motors emerged as a powerful device toward *in vivo* applications with biocompatibility, long lifetime, and on-demand motion control. The hydrogels placed into an acoustic field are usually passively driven by acoustic radiation force,[134] which does not necessarily cause the swelling of the hydrogel. Typically, the acoustic manipulation approaches utilize ultrasonic standing waves generated by piezoelectric transducers to propel, rotate, separate, or migrate micro/nanomotors.[135,136] Ahmed et al.[135] employed ultraviolet photopolymerization to fabricate rectangular PEG microswimmers with conical caves. After being submerged in liquid, bubbles were trapped in the caves, and the bubbles' oscillation in the acoustic field resulted in a steady flow field around the motor, which could propel it to move in a speed of 50 body lengths per second. Kaynak et al.[137] utilized a similar fabrication process to obtain PEG microswimmers with flagellum structures, and they found the speed of the microswimmers changed linearly from 200 to 1100 μm/s, depending on the voltage applied on the transducers. They further fabricated a much more delicate 3D hydrogel microswimmer by direct laser writing.[120] The microswimmer adopted a microjet engine structure, and the localized microstreaming around the tip of the conical wedge results in a jet in the middle of the device, which allowed it to propel itself or function as a microfluidic chamber.

Jumping is another powerful motion triggered by muscle-powered accelerations for many animals. Generally, the process first requires the muscle contraction to restore elastic potential energy and then a fast release of the stored elastic energy to produce kinetic energy.[138] Besides oscillation, photothermal induced bubble generation provides an opportunity to induce jumping by fast deformation of specific sites under light irradiation. Li et al.[67] synthesized a binary iron oxide nanoparticle (IONP) and poly(sodium acrylate) (pAANa) hydrogel sphere actuator. When irradiated by the side of the sphere, bubble generation occurred rapidly through the photothermal heating process and subsequently expanded the sphere within 800 ms and rebounded the hydrogel at a speed of 1.6 m/s to reach a jumping height of 15 cm (Figure 6h).

4. HYDROGEL MOTORS DRIVEN BY CHEMICAL FUELS OR EXTERNAL FIELDS

In the past decades, great endeavors have been made to create miniaturized "engines" that can convert stored chemical energy to controlled propulsion. In 2004, a pioneering work by Paxton and co-workers discovered the autonomous movement of Au−Pt bimetallic nanorods, which are propelled by self-electrophoresis.[5] Since then, micro/nanomotors with optimized materials, sizes, shapes, and propulsion mechanisms have been developed. Scientists have adopted various top-down or bottom-up fabrication techniques to obtain microengines in the forms of Janus particles,[38] rods,[121] core/shell droplets,[139] helices,[45,140] and tubes.[39] These miniaturized autonomous systems can efficiently convert chemical fuels (such as hydrogen peroxide,[141] hydrazine,[142] and glucose[143]) or external energy input (such as

https://doi.org/10.1021/acs.chemmater.2c01960
Chem. Mater. 2022, 34, 9307−9328

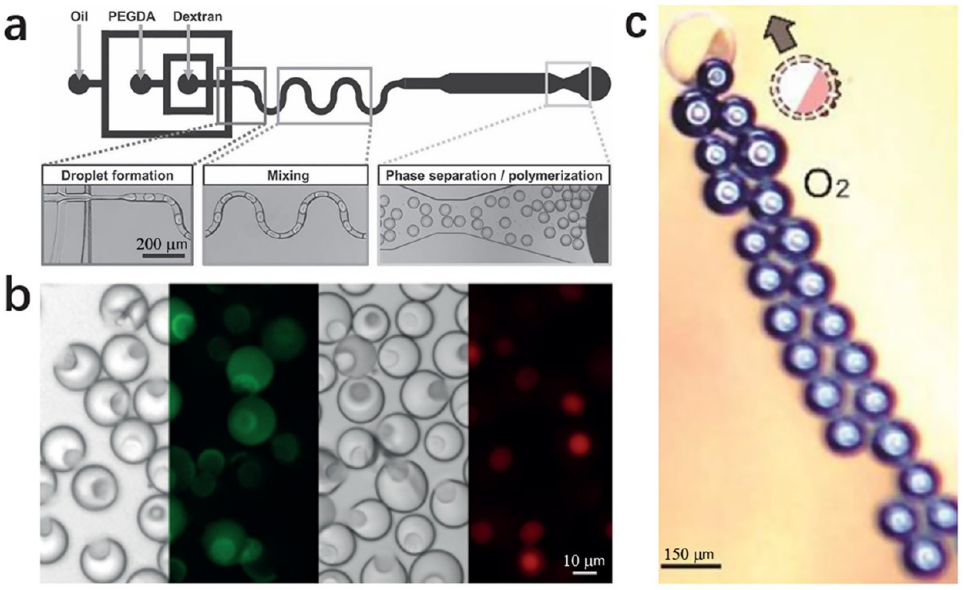

Figure 7. Catalytic motors driven by a bubble recoil mechanism. (a) Schematic of the microfluidic photolithography fabrication process. Reproduced with permission.[151] Copyright 2012, Wiley-VCH. (b) Two-phase-separating droplets consisting of a pEGDA capsule and dextran core. Reproduced with permission.[139] Copyright 2018, Wiley-VCH. (c) Bubble recoil of a Janus hydrogel particle deposited with Ti/Pt films. Reproduced with permission.[153] Copyright 2019, IOP Publishing Ltd.

magnetic energy,[141,144] ultrasonic energy,[145] optic energy,[146] thermal energy,[147] and electric energy[148]) to realize mechanical motion. Such micro/nanomotors are emerging as prominent candidates with their promising potential in diagnoses, *in vivo* drug delivery, sensing, and water purification.[149]

A comparison of different structures, mechanisms, and applications of hydrogel motors driven by chemical fuels or external fields is listed in Table 3. Much different from those stimuli-responsive hydrogel robotic systems, which generate spatiotemporal deformation profiles along their soft body to achieve directional movements, autonomous hydrogel motors discussed here are scarcely involved in deformation and thus require a different mechanism for their self-sustained locomotion. In this section, we review the structure, mechanism and design of nondeformed hydrogels in two broad categories on the basis of their distinct propulsion mechanisms, i.e., the autonomous chemical propulsion and external-stimuli-induced propulsion, and another type of hydrogel surface swimmers that move by the manipulation of local surface tension distribution.

4.1. Hydrogel Micro/Nanomotors Driven by Catalytic Bubble Recoil. Different catalysts have been embedded in hydrogel micromotors, such as inorganic particles including platinum (Pt),[141] MnO_2,[38] and $KMnO_4$[121] and biocatalysts including enzymes,[139] glucose oxidase,[143] and organic Prussian blue (PB) nanoparticles.[150] Like the stimuli-driven deformation regulated by anisotropic structures of hydrogel soft robots, the directional propulsion of micromotors requires the breakage of geometric symmetry. The key step is to fabricate hydrogel motors with smart structures for functionalization. Although various structures of hydrogel motors have been developed, the challenge remains in the scaled-up production of soft, biocompatible motors loaded with biocatalyst. In 2012, Ma et al.[151] proposed a selective polymerization of aqueous two-phase systems using glass capillary microfluidic devices (Figure 7a). During the fabrication, anisotropic spontaneous phase separation of microfluidic droplets containing two immiscible aqueous phases occurred, which resulted in droplet-in-droplet morphologies of controlled size, which upon polymerization leads to the desired asymmetrical gel particle. While traditional top-down lithography is labor-intensive and expensive, the microfluidic lithography approach that utilizes asymmetric, aqueous, and two-phase-separating droplets is very promising for its controllable size, morphology, low price, and ability for high-throughput fabrication.[151] This type of magnetic droplet could provide a magnetic torque of $\sim 6 \times 10^{-12}$ Nm in the presence of a rotating magnetic field.[152] Keller et al.[139] reported batch-fabricated microcapsule motors consisting of poly(ethylene glycol) diacrylate (pEGDA) and dextran with the biocatalyst enzyme placed in the pEGDA phase (Figure 7b). They studied the motion of the motor and found that the moving speed of the enzyme-mediated catalytic propulsion is influenced by the roughness of the motor, and the rougher surface allowed easier pinning of oxygen bubbles and thus high recoil speed.[139] Similarly, Liu et al. synthesized hydrogel microcapsules containing TiO_2 and ZnO NPs, which allowed the removal of the organic pollutant methylene blue through a photocatalytic process.[149]

A more classic anisotropic structure of hydrogel micromotors is the Janus particle with active catalysts coated or loaded on one side of the particle for bubble recoil. Lin et al.[38] employed a glass capillary microfluidic fabrication method to obtain hydrogel microspheres and then embedded functional NPs (MnO_2, Fe_3O_4, TiO_2) using photocurable hydrogel precursor to obtain Janus microspheres with different coverages. The catalytic reaction of hydrogen peroxide by NPs produced O_2 bubbles on the side coated with NPs, which resulted in directional propulsion. Zhu et al.[153] synthesized anhydride-derived hydrogel microcapsules by a microfluidic glass capillary device and further deposited Ti/Pt films with e-beam evaporation to obtain a Janus particle structure (Figure 7c). Their hydrogel motors are capable of permeation, purification, and separation of dissolved molecular species. Rods are another basic structure for efficient micromotors. Wang et al.[121] created emulsion-hydrogel soft motors templated from the oil/water emulsion. By simply

https://doi.org/10.1021/acs.chemmater.2c01960
Chem. Mater. 2022, 34, 9307−9328

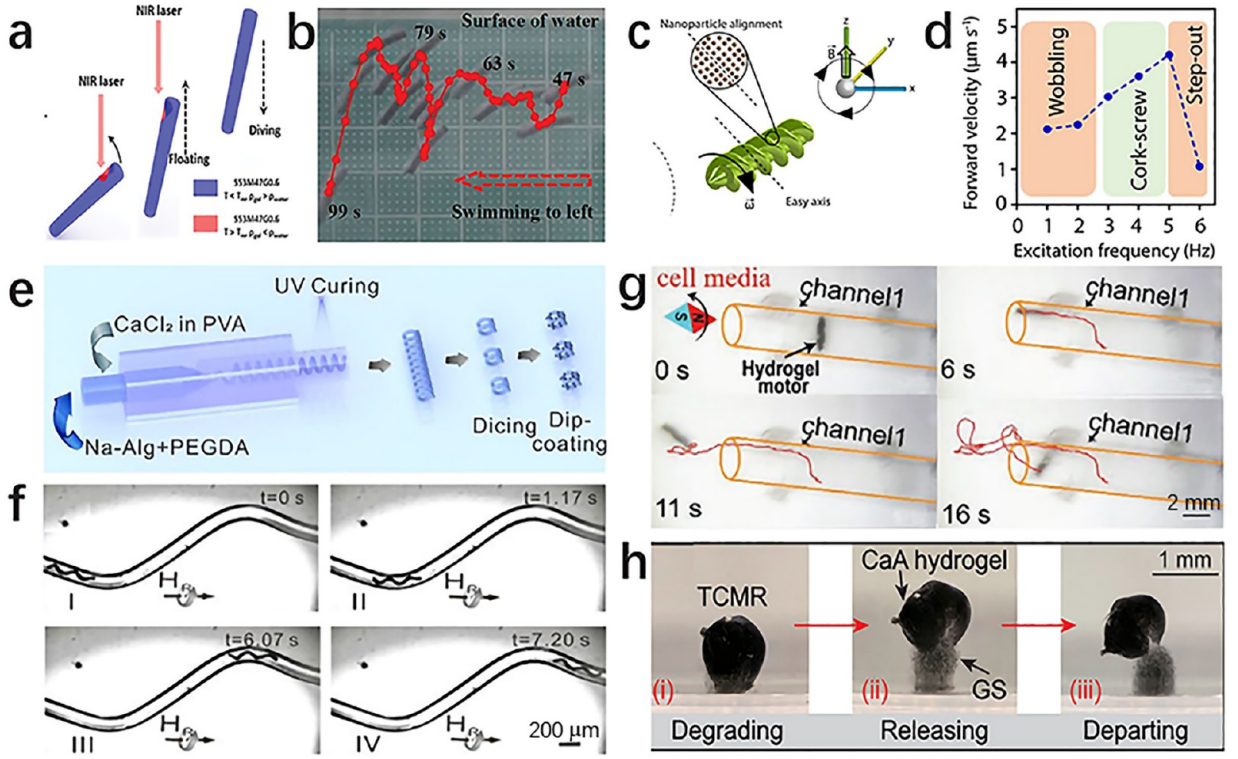

Figure 8. Hydrogel motors driven by external stimuli. (a) Mechanism of light-controlled diving/floating motion of a hydrogel tube. (b) Trajectory of depth-controllable directional swimming of a hydrogel tube. Reproduced with permission.[24] Copyright 2015, Wiley-VCH. (c) Schematic of a double-helical microswimmer loaded with aligned magnetic nanoparticles. (d) The step-out frequency of the microswimmer. Reproduced.[19] Copyright 2019, American Chemical Society. (e) Schematic of the synthesis process of hydrogel microhelices using a capillary microfluidic device. (f) Motion of a magnetic soft hydrogel helix to pass through a sinuous capillary. Reproduced with permission.[45] Copyright 2021, Elsevier. (g) Trajectories of helical motors passing through a constricted channel in cell media under a rotating magnetic field. Scale bars are 2 mm. Reproduced with permission.[154] Copyright 2021, Wiley-VCH. (h) Degradation and targeted drug release of a configurational microcapsule. Reproduced.[171] Copyright 2021, American Chemical Society.

injecting a saturated $KMnO_4$ catalytic solution in the tail of the hydrogel rod, self-propulsion through the catalytic reactions in H_2O_2 solutions occurs. A combination of the catalytic motor with other functional materials enriches the function of the motors. Hao et al.[150] reported a Prussian blue-reduced graphene oxide (PB-rGO) hydrogel self-propelling motor for water treatment, where the PB catalyzed H_2O_2 into oxygen bubbles to propel the motor and rGO catalyzed H_2O_2 into hydroxyl radicals as an oxidant for the degradation of pollutants. Zhu et al.[141] developed an artificial microfish loaded with Pt NPs on the tail for chemically mediated propulsion. A computer-controlled UV light cross-linking process assisted by the DMD device allowed precise loading of the ferromagnetic iron oxide particles on the head and thus magnetic steering of the moving direction during the bubble propulsion.

4.2. Hydrogel Micro/Nanomotors Driven by External Fields. Although chemical fuels are widely used to power catalytic micromotors, some toxic chemicals are not suitable for *in vivo* applications. Besides, the catalytic micromotors face challenges in increasing the degree of freedom in locomotion, improving the accuracy in positioning, and extending the functional durability. On the other hand, external stimuli-driven approaches utilizing light, magnetic field, ultrasound, etc. enable biocompatible manipulation and hold the potential to solve the problems above.[37,156] Unlike the hydrogel soft robots driven by stimuli-responsive deformation of the hydrogel itself, field-driven hydrogel motors are usually loaded with stimuli-responsive materials such as photothermal particles or magnetic particles to effectively convert external energy input into mechanical movements. Wang et al.[24] demonstrated the concept of a hydrogel microswimmer that is capable of diving and floating in water by controlling its density. The hydrogel is composed of two monomers, stearyl acrylate and methacrylic acid, as well as rGO as the NIR absorbent. Upon NIR light irradiation, the photothermal heating by rGO caused the melting−crystallization phase transition of the hydrogel. The density changes before and after the phase transition enabled the diving and floating of the microswimmer in water (Figure 8a). With real-time control of the irradiation time and direction, the swimming direction and the swimming depth could be instantaneously controlled (Figure 8b).[24]

One of the most efficient microrobots capable of overcoming viscous drag and propelling itself in a low Reynolds number regime is the magnetic artificial bacterial flagella (ABF).[157,158] The ABFs adopt a helical structure similar to that of the *Escherichia coli* bacteria, which could be made by rolled-up technology,[159] a template,[160] direct laser writing,[161] and microfluidic lithography.[45,140] In a rotary magnetic field, the ABFs rotate around their axial direction and thus cause a unique cork-screw propulsion. Ceylan et al.[19] fabricated a double-helical microswimmer by two-photon microprinting. During the printing, the iron oxide nanoparticles dispersed in the photocurable precursor gelatin methacryloyl were aligned by the magnetic field and thus enabled the field-driven locomotion in fluidic environments (Figure 8c). They studied the movement of the microswimmer with increased rotational frequency of the

https://doi.org/10.1021/acs.chemmater.2c01960
Chem. Mater. 2022, 34, 9307−9328

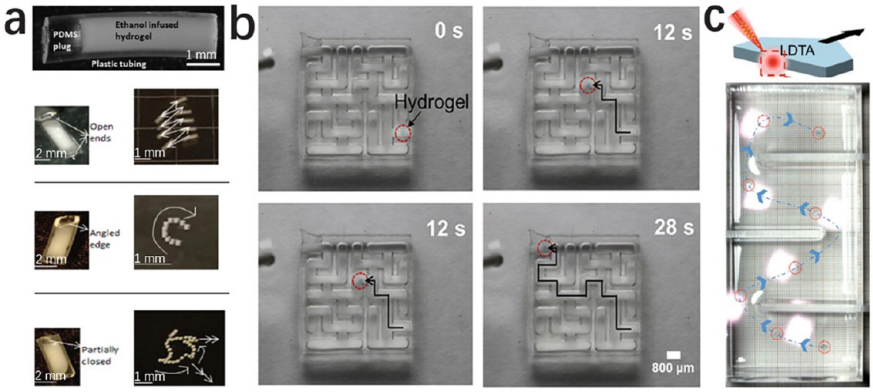

Figure 9. Surface swimming hydrogel robots that propel by the manipulation of local surface tension distribution. (a) Structure of a hydrogel robot infused with ethanol and its different trajectories generated by different designs. Reproduced.[173] Copyright 2012, American Chemical Society. (b) Image sequences of the hydrogel passing through a microfluidic maze with a composition gradient. Reproduced.[42] Copyright 2012, American Chemical Society. (c) Directional motions of a hydrogel swimmer driven by a photothermal induced Marangoni effect. Reproduced with permission.[41] Copyright 2021 Wiley-VCH.

magnetic field. The typical swimming behavior of magnetic ABFs is divided into wobbling, cork-screw, and step-out regions with increased frequency.[158] The forward velocity of the microswimmer increased linearly in the cork-screw region and reached its maximum before the step-out region (Figure 8d).[19] Liu et al.[45] combined microfluidic photolithography with a dip-coating process to generate a soft helical structure loaded with magnetic nanoparticles (Figure 8e). The mechanical property of the helix can be finely tuned by adjusting the pEGDA percentage in materials followed by treatment in Na^+/Ca^{2+} solutions. With the low modulus of the soft body, the obtained magnetic helix was capable of being actively propelled through narrow and sinuous microchannels by a magnetic torque of 3.29×10^{-13} Nm exerted by a rotating magnetic field, mimicking the deformability of living cells (Figure 8f).[45] In addition, Huang et al.[157] combined magnetic programming and photolithography to aligned magnetic nanoparticles in layered hydrogel ABFs. This unique design allowed programmable shape morphing of the microrobots and thus controllable motility. The motility and maneuverability of their ABFs can also be adjusted on demand by dynamically remagnetizing the body by applying a magnetic field significantly higher than the magnetic field applied to align the magnetic nanoparticles during the fabrication process.[158]

When a magnetic microrobot is levitated in biomedical liquids, the Earnshaw's theorem implies that a stable position of the micromotor cannot be maintained by the stationary magnetic force.[162] Therefore, a feedback control is needed to accurately hold the position and pose of the microrobot. A five-degree-of-freedom (5-DOF) electromagnetic microrobot operation system, OctoMag, was proposed in 2010, which enables autonomous and precise control over the motion of magnetic micromotors by computer vision.[163] Fusco et al.[164] further utilized this system to control and plan the trajectory of a hydrogel micromotor loaded with magnetic beads. A visual tracker allowed the recognition of selected magnetic beads. and the controller of the magnetic field generated a suitable field strength, frequency, and direction to move the beads along the preplanned trajectory.

Although the propulsion with external fields is biocompatible, it still raises concerns about the toxicity of the motor and rejection reactions if the foreign object cannot be expelled from the human body. From this perspective, it is necessary to form hydrogel motors with fully biodegradable materials for *in vivo* applications, which allows noninvasive material removal after targeted interventions.[164−166] Peters et al.[30] reported a one-step fabrication of a biodegradable hydrogel helix loaded with superparamagnetic particles. The magnetic composites were cross-linked via single- and two-photon polymerization of a mixture of pEGDA and pentaerythritol triacrylate (PETA) with Fe_3O_4 nanoparticles. The polymer network was able to absorb and deliver targeted drugs to fibroblast cells and then degrade in physiological environments. A similar 3D laser lithography approach is adopted by Sun et al.[167] to form a biodegradable hydrogel motor propelled by an oscillating magnetic field. Instead of the helix, they designed a special structure composed of four rigid segments connected by flexible springs, which allowed undulation locomotion that propelled them in the low Reynolds number regime. The main construction material pEGDA is approved by the Food and Drug Administration (FDA) for human use, which also satisfies the biodegradability requirement for real-time *in vivo* applications.[167] While techniques like 3D laser writing or glance angle deposition require expensive and complex instruments, Wang et al.[154] proposed a versatile fabrication setup to produce a biocompatible helical PVA hydrogel motor. Instead of 3D printing, they employed a rotary machine that attached to a silk-like hydrogel mixture of PVA and Fe_3O_4 NPs to fabricate the helix and then used photocuring to solidify the structure; the obtained helix was able to penetrate constricted channels in cell media under a rotating magnetic field (Figure 8g).[154] Besides the hydrogel motors mentioned above, other micromotors made by biodegradable materials such as gelatin methacryloyl (GelMA),[131] sugar,[168] zwitterionic photoresists,[166] proteins,[169] and metal−organic frameworks (MOFs)[170] can be found in the literature.

Active targeted therapy using untethered micromotors is a challenging task, which requires the locomotion of the motor toward the target and controllable release of the loaded drugs. Chen et al.[171] designed a configurational microcapsule that enabled targeted delivery of the anticancer therapeutic doxorubicin (DOX). Their microcapsule consists of a multilevel structure of a calcium alginate (CaA) magnetic hydrogel, gelatin sphere, and core of chitosan microspheres loaded with drugs. The three parts are severed for locomotion, seeding of biological tissue, and drug release, respectively (Figure 8h).[171] Besides biomedical applications, the bottom-up assembly of colloidal−

https://doi.org/10.1021/acs.chemmater.2c01960
Chem. Mater. 2022, 34, 9307−9328

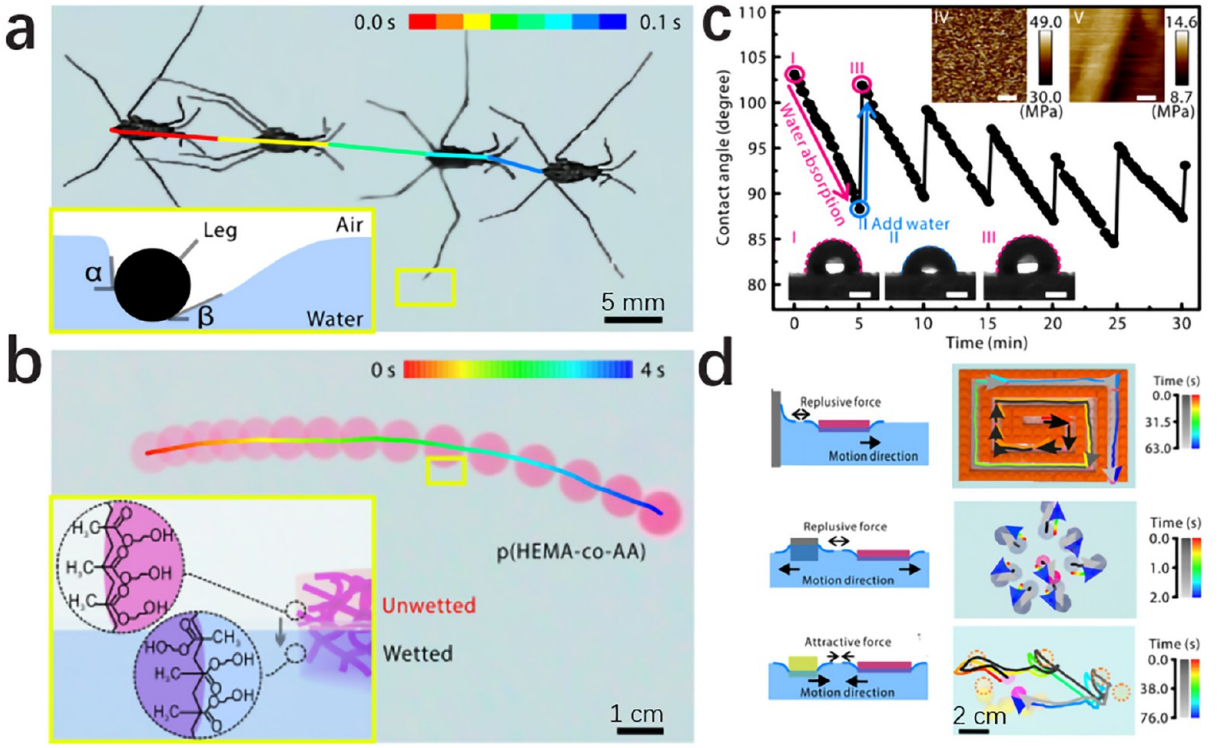

Figure 10. Hydrogel water striders autonomously move on the water surface without operated stimuli. (a) Trajectory of a water strider in 0.1 s. The inset is a schematic illustration of the propulsion mechanism of a water strider. (b) Trajectory of a hydrogel swimming on the water surface in 4 s. The inset is a schematic illustration of the propulsion mechanism of a hydrogel water strider. (c) Contact angle changes on the hydrogel surface within 30 min. Scale bars are 1mm (bottom inset) and 100 nm (top inset). (d) Trajectory of the hydrogel swimmer with a dynamic interaction with the surroundings and objects of different hydrophilic/hydrophobic properties. Reproduced with permission.[43] Copyright 2021, AAAS.

hydrogel devices is of interest to obtain highly controllable structures and thus novel functionalities. Peng et al.[146] proposed a colloidal assembly system on the basis of light-assisted thermophoresis propulsion. Instead of guiding the motion of the hydrogel itself, the hydrogel solution could be an ideal matrix for optothermal manipulation. With a light-induced localized temperature increase in the hydrogel solution, they created a thermoelectric field and depleted attraction force to actively manipulate the suspended colloidal particles of sizes smaller than 5 μm.[146]

4.3. Surface Tension-Driven Autonomous Hydrogel Robots. Insects such as water striders *Mesovelia* and beetle larvae *Pyrrhalta*[40] move on the water surface by agilely controlling the curvature of the water surface. Inspired by these creatures, hydrogel robots that move through the manipulation of local surface tension are of interest as another class of intelligent autonomous devices. Most of them are driven by the local variation of surface tension and corresponding fluid motion caused by composition or temperature gradients, i.e., the Marangoni effect.[172] Sharma et al.[173] encapsulated an ethanol-containing PAA hydrogel within polydimethylsiloxane (PDMS) and designed openings at different positions to allow diffusion of ethanol into the water surroundings. With a specific structure, ethanol with a surface tension lower than that of water leaked from one side, and thus, a surface tension gradient that propelled the swimmer toward regions with higher surface tension, i.e., lower ethanol concentration, was formed. Such swimmers exhibited long motion duration and tunable trajectories by changing the opening positions (Figure 9a).[173]

Instead of loading chemicals in the hydrogel swimmer, Wang et al. investigated the locomotion of the hydrogel sphere driven by concentration gradients in the environment. The hydrogel sphere is able to smartly navigate through a maze where the gradient of surface tension is formed by a drop of ethanol at the exit (Figure 9b).[42] A limitation of the design of such a concentration gradient based on the Marangoni effect is that the propulsion only lasts when the "fuel" is available or when a concentration gradient is built up in the environment. An alternative is to actively generate a thermal gradient around the hydrogel, which changes the local surface tension of water. Pan et al.[41] reported a transparent hydrogel swimmer that can perform not only directional propulsion but also floating–sinking 3D motions under the NIR laser beam irradiation or sunlight. The hydrogel was composed of pNIPAm embedded with photothermal CuS nanoparticles (Figure 9c). The photothermal heating changed the surrounding surface tension and drove the motion of the hydrogel. Moreover, the porous hydrogel could sink by absorbing liquid molecules and then float by the buoyant flow under NIR irradiation.

Although the above Marangoni effect-driven surface swimmers have shown intelligence to find chemical cues in a complex space and are capable of omnidirectional movement, they require the addition of surfactants to produce chemical gradients in the environment or operated stimuli to actively generate thermal gradients. The water striders in nature are self-sustained and use repeated strikes of their middle legs to manipulate the local curvature of the water surface and to propel in a periodic manner (Figure 10a). Inspired by water striders, our group has recently proposed a novel dynamic wetting mechanism that enables hydrogels to achieve non-deformed, stimulus-free, and autonomous swimming on the water surface (Figure 10b).[43] The synthesized poly(hydroxyethyl methacrylate-*co*-acrylic

https://doi.org/10.1021/acs.chemmater.2c01960
Chem. Mater. 2022, 34, 9307−9328

acid) [p(HEMA-*co*-AA)] hydrogel could move autonomously on the water surface for a duration as long as 210 min without any human intervention or external energy input. The typical compositions of hydrogels consisted of long carbon chains with hydrophilic hydroxyl groups on the side chains and hydrophobic methyl groups on the backbone. When the pristine hydrogel was placed in the air, it preferentially exposed the nonpolar parts of the backbone toward the air to minimize surface energy. During this process, the pristine hydrogel was unwetted. When submerged in water, the hydroxyl groups migrated to the surface to minimize the interfacial free energy. In the water absorption process, the reorientation of the hydrophobic and hydrophilic groups occurred at the outermost interface. Subsequently, the partially wetted hydrogel exposed new unwetted parts to water because it sank slightly into the water, and this repeated process is named dynamic wetting, as evidenced by the repeated contact angle change on the hydrogel surface measured in a period of 30 min (Figure 10c).[43]

The dynamic wetting phenomenon occurring at the water−air interface resulted in a spacial-temporal-varying distribution of surface tension. Due to the anisotropy in shapes, the partially wetted hydrogel moved toward the unwetted region with a fluctuated velocity. When swimming autonomously on the water surface, the unevenly distributed surface tension around the hydrogels allowed them to adaptively interact with surroundings and objects of different hydrophilic/hydrophobic properties and thus accomplish different tasks.[43] When placed in a maze with a hydrophilic boundary, the hydrogel repelled itself from the boundary and moved with a wall-following trajectory that guided it to the exit. When surrounded by hydrophilic thermoplastic polyurethane membranes, the hydrogel expelled all the obstacles and escaped from them; on the contrary, the hydrogel would get close to and collect hydrophobic PDMS balls (Figure 10d). Besides the p(HEMA-*co*-AA) hydrogel, other types of acrylic derivative hydrogels such as pHEMA and poly(methacrylic acid) (pMA) showed similar locomotion capability, and their movement duration is closely related to the static equilibrium swelling time.[43] When a gradient or bilayer structure was employed, the p(HEMA-*co*-AA) hydrogel exhibited a humidity-responsive shape morphing behavior. When incorporated with active elements such as *N*-isopropylacrylamide (NIPAM), acrylic acid, azobenzene, or 2-acrylamido-2-methylpropanesulfonic acid (AMPS), it rendered the hydrogel temperature-, pH-, light-, or electrical-responsive behaviors, which further increased the degree of freedom in manipulating the hydrogel's locomotion and functionality.

While the existing self-propelled autonomous hydrogel-based devices still rely on chemical fuels or external energy input by stimuli to form bubble propulsion or phoresis propulsion, the autonomous locomotion induced by dynamic wetting involves no toxic chemicals or operated stimuli. Such an advantage in this self-propelling technology could easily be applied to harness environmental pollution, cargo transport and delivery, and autonomous monitoring with minimal human operation.

5. CONCLUSION AND OUTLOOK

In summary, researchers have made great endeavors in the development of hydrogel actuators that can convert external environmental stimuli into their motion, and the pursuit of achieving dynamic, robust, and adaptable manipulations has pushed forward the establishment of novel design principles and strategies. The osmotic-driven motion of hydrogel mimicking natural plants brought about its advantages in softness, stimuli-responsive properties, and programmability but also drawbacks in its long response time and limited actuation force. Interestingly, the recent advances in the anisotropic structure fabrication, composite design, and multiresponsive manipulation have helped to overcome the challenges in the intrinsic limits of hydrogels and thus broaden their applications to various fields.

Diverse strategies have been adopted to translate natural principles into technological capabilities in the two distinct hydrogel robotic systems, i.e., the hydrogel soft robots driven by stimuli-sensitive swelling deformation and the hydrogel motors powered by catalytic bubble recoil or external fields. In the deformation-driven hydrogel soft robots, the key is to integrate effective onboard energy conversion mechanisms and to actively control the shape morphing upon external stimuli. The embedment of superior photoresponsive materials into the robot's soft bodies has made them efficient machines to perform deformations with high frequency, large force, and high speed. On the other hand, the dominating strategy of hydrogel motors is the combination of anisotropic structures with self-sustained propelling mechanisms. The advancement of high-throughput fabrication with biodegradable materials has allowed the batch synthesis of highly structured capsules, helices, and droplets that are applicable for *in vivo* drug delivery and therapies. Among them, the nonreciprocal propulsion by the magnetic field makes them competent to penetrate complex fluidic environments with low Reynolds numbers. Moreover, novel mechanisms of fully autonomous hydrogel surface swimmers have further opened the possibility of artificial devices with minimal human operation. These design principles are critical to develop hydrogel soft robots and motors that can exceed current engineering practices and perform with animal-like agility, maneuverability, and dexterity. The future development of hydrogel robotic systems will rely on the in-depth understanding of the mechanism of living organisms, novel functional materials, multiscale structural designs, and configurable morphologies.

Additionally, further improvements of hydrogel robots will depend on the integration of new materials and new designs with close-loop feedback mechanisms that allow improved intelligence, adaptability, biocompatibility, and multifunctionality. First of all, the discovery of new materials will enable the synthesis of fully soft, biocompatible, biodegradable, and multifunctional hydrogel robots. The utilization of biofuels such as glucose, adenosine triphosphoric acid, and protein will expand the application of autonomous hydrogel robots in biological environments and significantly improve their competence of fulfilling various biological tasks. Second, advanced fabrication technologies such as 4D printing should be combined with theoretical modeling to design predicable shape morphing and predesigned transformation. Third, the buildup of close-loop feedbacks within miniaturized soft robots remains a challenge. The key is to embed the controlling system with machine learning. The system should be able to transform data collected during the tour of the robot into next-step actuation commands and help deliver clinically meaningful information of the human body for the detection, diagnosis, and characterization of human diseases.

AUTHOR INFORMATION

Corresponding Author

Yongfeng Mei − *Department of Materials Science & State Key Laboratory of Molecular Engineering of Polymers, Fudan University, Shanghai 200438, People's Republic of China;*

https://doi.org/10.1021/acs.chemmater.2c01960
Chem. Mater. 2022, 34, 9307−9328

Shanghai Frontiers Science Research Base of Intelligent Optoelectronics and Perception, Institute of Optoelectronics and International Institute of Intelligent Nanorobots and Nanosystems, Fudan University, Shanghai 200438, People's Republic of China; Yiwu Research Institute of Fudan University, Yiwu 322000 Zhejiang, People's Republic of China; orcid.org/0000-0002-3314-6108; Email: yfm@fudan.edu.cn

Authors

Yi Ouyang − *Department of Materials Science & State Key Laboratory of Molecular Engineering of Polymers, Fudan University, Shanghai 200438, People's Republic of China; Shanghai Frontiers Science Research Base of Intelligent Optoelectronics and Perception, Institute of Optoelectronics and International Institute of Intelligent Nanorobots and Nanosystems, Fudan University, Shanghai 200438, People's Republic of China; Yiwu Research Institute of Fudan University, Yiwu 322000 Zhejiang, People's Republic of China*

Gaoshan Huang − *Department of Materials Science & State Key Laboratory of Molecular Engineering of Polymers, Fudan University, Shanghai 200438, People's Republic of China; Shanghai Frontiers Science Research Base of Intelligent Optoelectronics and Perception, Institute of Optoelectronics and International Institute of Intelligent Nanorobots and Nanosystems, Fudan University, Shanghai 200438, People's Republic of China; Yiwu Research Institute of Fudan University, Yiwu 322000 Zhejiang, People's Republic of China;* orcid.org/0000-0002-0525-7177

Jizhai Cui − *Department of Materials Science & State Key Laboratory of Molecular Engineering of Polymers, Fudan University, Shanghai 200438, People's Republic of China; Shanghai Frontiers Science Research Base of Intelligent Optoelectronics and Perception, Institute of Optoelectronics and International Institute of Intelligent Nanorobots and Nanosystems, Fudan University, Shanghai 200438, People's Republic of China; Yiwu Research Institute of Fudan University, Yiwu 322000 Zhejiang, People's Republic of China*

Hong Zhu − *Department of Materials Science & State Key Laboratory of Molecular Engineering of Polymers, Fudan University, Shanghai 200438, People's Republic of China; Shanghai Frontiers Science Research Base of Intelligent Optoelectronics and Perception, Institute of Optoelectronics and International Institute of Intelligent Nanorobots and Nanosystems, Fudan University, Shanghai 200438, People's Republic of China; Yiwu Research Institute of Fudan University, Yiwu 322000 Zhejiang, People's Republic of China*

Guanghui Yan − *Department of Materials Science & State Key Laboratory of Molecular Engineering of Polymers, Fudan University, Shanghai 200438, People's Republic of China; Shanghai Frontiers Science Research Base of Intelligent Optoelectronics and Perception, Institute of Optoelectronics and International Institute of Intelligent Nanorobots and Nanosystems, Fudan University, Shanghai 200438, People's Republic of China; Yiwu Research Institute of Fudan University, Yiwu 322000 Zhejiang, People's Republic of China*

Complete contact information is available at: https://pubs.acs.org/10.1021/acs.chemmater.2c01960

Notes

The authors declare no competing financial interest.

Biographies

Yi Ouyang received his Ph.D. degree in materials physics and chemistry in 2020 from the Ningbo Institute of Materials Technology and Engineering, Chinese Academy of Sciences. He is currently a postdoctoral researcher mentored by Prof. Yongfeng Mei in the Department of Materials Science, Fudan University. His research interest focuses on magnetic soft robots with light-induced magnetic transitions toward biological applications.

Gaoshan Huang is a Professor in the Department of Materials Science, Fudan University. He obtained his B.S. and Ph.D. in condensed matter physics from Nanjing University. He completed postdoctoral fellowships at the Leibniz Institute for Solid State and Materials Research, Dresden, and the Institute of Materials Research and Engineering, Singapore. His current research interests are nanomembranes and their assembled structures for optoelectronic applications.

Jizhai Cui is an Associate Professor at the Department of Materials Science, Fudan University. He received his Ph.D. degree in 2016 from the University of California, Los Angeles. From 2016 to 2020, he conducted postdoctoral research at ETH Zurich and Paul Scherrer Institute in Switzerland. His research interest includes micro- and nanorobots and ferroelectric and ferromagnetic materials and devices.

Hong Zhu received her Ph.D. degree in 2022 from the Department of Materials Science, Fudan University. She is a postdoctoral researcher right now. Her research interest includes hydrogel-based micromotors and soft robots.

Guanghui Yan received his Ph.D. degree in materials physics and chemistry in 2019 from Ningbo Institute of Materials Technology and Engineering, Chinese Academy of Sciences. He is currently a postdoctoral researcher mentored by Prof. Yongfeng Mei in the Department of Materials Science, Fudan University. His research interest is focused on ferromagnetic nanomembranes and micromotors.

Yongfeng Mei received his B.S. and M.S. in physics from Nanjing University and Ph.D. in materials physics from City University of Hong Kong. He is a professor in materials physics and the deputy dean in the Department of Materials Science at Fudan University (China). Before that, he worked as a postdoctoral researcher in the Max Planck Institute for Solid State Research (Germany) and then led a research group in the Leibniz Institute for Solid State and Materials Research Dresden (Germany) as a staff scientist. His research interest focuses on micro/nanorobotics, flexible electronics/optoelectronics, and nanophotonics.

■ ACKNOWLEDGMENTS

This work was supported by the National Natural Science Foundation of China (nos. 51961145108, 61975035, and 62005050), the Project funded by the China Postdoctoral Science Foundation (no. 2021M700785), and the Program of Shanghai Academic Research Leader (no. 19XD1400600).

■ REFERENCES

(1) Liu, X.; Liu, J.; Lin, S.; Zhao, X. Hydrogel Machines. *Mater. Today* **2020**, *36*, 102−124.
(2) Wang, X. Q.; Ho, G. W. Design of Untethered Soft Material Micromachine for Life-Like Locomotion. *Mater. Today* **2022**, *53*, 197−216.
(3) Chen, X. Z.; Hoop, M.; Mushtaq, F.; Siringil, E.; Hu, C.; Nelson, B. J.; Pané, S. Recent Developments in Magnetically Driven Micro- and Nanorobots. *Appl. Mater. Today* **2017**, *9*, 37−48.
(4) Lin, X.; Xu, B.; Zhu, H.; Liu, J.; Solovev, A.; Mei, Y. Requirement and Development of Hydrogel Micromotors towards Biomedical Applications. *Research* **2020**, *2020*, 7659749.
(5) Paxton, W. F.; Kistler, K. C.; Olmeda, C. C.; Sen, A.; St. Angelo, S. K.; Cao, Y.; Mallouk, T. E.; Lammert, P. E.; Crespi, V. H. Catalytic

Nanomotors: Autonomous Movement of Striped Nanorods. *J. Am. Chem. Soc.* **2004**, *126*, 13424−13431.
(6) Wichterle, O.; LÍM, D. Hydrophilic Gels for Biological Use. *Nature* **1960**, *185*, 117−118.
(7) Saroia, J.; Yanen, W.; Wei, Q.; Zhang, K.; Lu, T.; Zhang, B. A Review on Biocompatibility Nature of Hydrogels with 3D Printing Techniques, Tissue Engineering Application and Its Future Prospective. *Bio-Des. Manuf.* **2018**, *1*, 265−279.
(8) Ionov, L. Biomimetic Hydrogel-Based Actuating Systems. *Adv. Funct. Mater.* **2013**, *23*, 4555−4570.
(9) Erol, O.; Pantula, A.; Liu, W.; Gracias, D. H. Transformer Hydrogels: A Review. *Adv. Mater. Technol.* **2019**, *4*, 1900043.
(10) Blanco-Fernandez, B.; Gaspar, V. M.; Engel, E.; Mano, J. F. Proteinaceous Hydrogels for Bioengineering Advanced 3D Tumor Models. *Adv. Sci.* **2021**, *8*, 2003129.
(11) Zhu, J.; Marchant, R. E. Design Properties of Hydrogel Tissue-Engineering Scaffolds. *Expert Rev. Med. Devices* **2011**, *8*, 607−626.
(12) Vegas, A. J.; Veiseh, O.; Doloff, J. C.; Ma, M.; Tam, H. H.; Bratlie, K.; Li, J.; Bader, A. R.; Langan, E.; Olejnik, K.; Fenton, P.; Kang, J. W.; Hollister-Locke, J.; Bochenek, M. A.; Chiu, A.; Siebert, S.; Tang, K.; Jhunjhunwala, S.; Aresta-Dasilva, S.; Dholakia, N.; Thakrar, R.; Vietti, T.; Chen, M.; Cohen, J.; Siniakowicz, K.; Qi, M.; McGarrigle, J.; Graham, A. C.; Lyle, S.; Harlan, D. M.; Greiner, D. L.; Oberholzer, J.; Weir, G. C.; Langer, R.; Anderson, D. G. Combinatorial Hydrogel Library Enables Identification of Materials that Mitigate the Foreign Body Response in Primates. *Nat. Biotechnol.* **2016**, *34*, 345−352.
(13) Liu, Y.; Yang, T.; Zhang, Y.; Qu, G.; Wei, S.; Liu, Z.; Kong, T. Ultrastretchable and Wireless Bioelectronics Based on All-Hydrogel Microfluidics. *Adv. Mater.* **2019**, *31*, No. e1902783.
(14) Cosson, S.; Lutolf, M. P. Hydrogel Microfluidics for the Patterning of Pluripotent Stem Cells. *Sci. Rep.* **2015**, *4*, 4462.
(15) Kang, D. H.; Kim, S. M.; Lee, B.; Yoon, H.; Suh, K. Y. Stimuli-Responsive Hydrogel Patterns for Smart Microfluidics and Microarrays. *Analyst* **2013**, *138*, 6230−6242.
(16) Kim, Y.; Parada, G. A.; Liu, S.; Zhao, X. Ferromagnetic Soft Continuum Robots. *Sci. Robot.* **2019**, *4*, No. eaax7329.
(17) Chen, Y.; Yang, J.; Zhang, X.; Feng, Y.; Zeng, H.; Wang, L.; Feng, W. Light-Driven Bimorph Soft Actuators: Design, Fabrication, and Properties. *Mater. Horiz.* **2021**, *8*, 728−757.
(18) Harrington, M. J.; Razghandi, K.; Ditsch, F.; Guiducci, L.; Rueggeberg, M.; Dunlop, J. W.; Fratzl, P.; Neinhuis, C.; Burgert, I. Origami-Like Unfolding of Hydro-Actuated Ice Plant Seed Capsules. *Nat. Commun.* **2011**, *2*, 337−343.
(19) Ceylan, H.; Yasa, I. C.; Yasa, O.; Tabak, A. F.; Giltinan, J.; Sitti, M. 3D-Printed Biodegradable Microswimmer for Theranostic Cargo Delivery and Release. *ACS Nano* **2019**, *13*, 3353−3362.
(20) Hill, B. S.; Findlay, G. P. The Power of Movement in Plants: the Role of Osmotic Machines. *Q. Rev. Biophys.* **1981**, *14*, 173−222.
(21) Li, Z.; Myung, N. V.; Yin, Y. Light-Powered Soft Steam Engines for Self-Adaptive Oscillation and Biomimetic Swimming. *Sci. Robot.* **2021**, *6*, No. eabi4523.
(22) Zhu, Q. L.; Du, C.; Dai, Y.; Daab, M.; Matejdes, M.; Breu, J.; Hong, W.; Zheng, Q.; Wu, Z. L. Light-Steered Locomotion of Muscle-Like Hydrogel by Self-Coordinated Shape Change and Friction Modulation. *Nat. Commun.* **2020**, *11*, 5166.
(23) Xiang, S. L.; Su, Y. X.; Yin, H.; Li, C.; Zhu, M. Q. Visible-Light-Driven Isotropic Hydrogels as Anisotropic Underwater Actuators. *Nano Energy* **2021**, *85*, 105965.
(24) Wang, L.; Liu, Y.; Cheng, Y.; Cui, X.; Lian, H.; Liang, Y.; Chen, F.; Wang, H.; Guo, W.; Li, H.; Zhu, M.; Ihara, H. A Bioinspired Swimming and Walking Hydrogel Driven by Light-Controlled Local Density. *Adv. Sci.* **2015**, *2*, 1500084.
(25) Shin, Y.; Choi, M. Y.; Choi, J.; Na, J. H.; Kim, S. Y. Design of an Electro-Stimulated Hydrogel Actuator System with Fast Flexible Folding Deformation under a Low Electric Field. *ACS Appl. Mater. Interfaces* **2021**, *13*, 15633−15646.
(26) Chen, Z.; Liu, J.; Chen, Y.; Zheng, X.; Liu, H.; Li, H. Multiple-Stimuli-Responsive and Cellulose Conductive Ionic Hydrogel for Smart Wearable Devices and Thermal Actuators. *ACS Appl. Mater. Interfaces* **2021**, *13*, 1353−1366.
(27) Zheng, W. J.; An, N.; Yang, J. H.; Zhou, J.; Chen, Y. M. Tough Al-Alginate/Poly(N-isopropylacrylamide) Hydrogel with Tunable LCST for Soft Robotics. *ACS Appl. Mater. Interfaces* **2015**, *7*, 1758−1764.
(28) Therien-Aubin, H.; Wu, Z. L.; Nie, Z.; Kumacheva, E. Multiple Shape Transformations of Composite Hydrogel Sheets. *J. Am. Chem. Soc.* **2013**, *135*, 4834−4839.
(29) Li, C.; Lau, G. C.; Yuan, H.; Aggarwal, A.; Dominguez, V. L.; Liu, S.; Sai, H.; Palmer, L. C.; Sather, N. A.; Pearson, T. J.; Freedman, D. E.; Amiri, P. K.; de la Cruz, M. O.; Stupp, S. I. Fast and Programmable Locomotion of Hydrogel-Metal Hybrids under Light and Magnetic Fields. *Sci. Robot.* **2020**, *5*, No. eabb9822.
(30) Peters, C.; Hoop, M.; Pane, S.; Nelson, B. J.; Hierold, C. Degradable Magnetic Composites for Minimally Invasive Interventions: Device Fabrication, Targeted Drug Delivery, and Cytotoxicity Tests. *Adv. Mater.* **2016**, *28*, 533−538.
(31) Kobayashi, K.; Yoon, C.; Oh, S. H.; Pagaduan, J. V.; Gracias, D. H. Biodegradable Thermomagnetically Responsive Soft Untethered Grippers. *ACS Appl. Mater. Interfaces* **2019**, *11*, 151−159.
(32) Goudu, S. R.; Yasa, I. C.; Hu, X.; Ceylan, H.; Hu, W.; Sitti, M. Biodegradable Untethered Magnetic Hydrogel Milli-Grippers. *Adv. Funct. Mater.* **2020**, *30*, 2004975.
(33) Wang, E.; Desai, M. S.; Lee, S. W. Light-Controlled Graphene-Elastin Composite Hydrogel Actuators. *Nano Lett.* **2013**, *13*, 2826−2830.
(34) Wu, Z. L.; Moshe, M.; Greener, J.; Therien-Aubin, H.; Nie, Z.; Sharon, E.; Kumacheva, E. Three-Dimensional Shape Transformations of Hydrogel Sheets Induced by Small-Scale Modulation of Internal Stresses. *Nat. Commun.* **2013**, *4*, 1586−1593.
(35) Maeda, S.; Hara, Y.; Sakai, T.; Yoshida, R.; Hashimoto, S. Self-Walking Gel. *Adv. Mater.* **2007**, *19*, 3480−3484.
(36) Shiraki, Y.; Akimoto, A. M.; Miyata, T.; Yoshida, R. Autonomous Pulsatile Flow by Peristaltic Motion of Tubular Self-Oscillating Gels. *Chem. Mater.* **2014**, *26*, 5441−5443.
(37) Wang, K.; Ren, J.; Yang, S.; Wang, H. Hydrogel-Based Motors. *Adv. Mater. Technol.* **2021**, *6*, 2100158.
(38) Lin, X.; Zhu, H.; Zhao, Z.; You, C.; Kong, Y.; Zhao, Y.; Liu, J.; Chen, H.; Shi, X.; Makarov, D.; Mei, Y. Hydrogel-Based Janus Micromotors Capped with Functional Nanoparticles for Environmental Applications. *Adv. Mater. Technol.* **2020**, *5*, 2000279.
(39) Wang, H.; Liang, Y.; Gao, W.; Dong, R.; Wang, C. Emulsion Hydrogel Soft Motor Actuated by Thermal Stimulation. *ACS Appl. Mater. Interfaces* **2017**, *9*, 43211−43219.
(40) Hu, D. L.; Bush, J. W. Meniscus-Climbing Insects. *Nature* **2005**, *437*, 733−736.
(41) Pan, D.; Wu, D.; Li, P. J.; Ji, S. Y.; Nie, X.; Fan, S. Y.; Chen, G. Y.; Zhang, C. C.; Xin, C.; Xu, B.; Zhu, S.; Cai, Z.; Hu, Y.; Li, J.; Chu, J. Transparent Light-Driven Hydrogel Actuator Based on Photothermal Marangoni Effect and Buoyancy Flow for Three-Dimensional Motion. *Adv. Funct. Mater.* **2021**, *31*, 2009386.
(42) Wang, Y.; Liu, X.; Li, X.; Wu, J.; Long, Y.; Zhao, N.; Xu, J. Directional and Path-Finding Motion of Polymer Hydrogels Driven by Liquid Mixing. *Langmuir* **2012**, *28*, 11276−11280.
(43) Zhu, H.; Xu, B.; Wang, Y.; Pan, X.; Qu, Z.; Mei, Y. Self-Powered Locomotion of a Hydrogel Water Strider. *Sci. Robot.* **2021**, *6*, No. eabe7925.
(44) Kagan, D.; Benchimol, M. J.; Claussen, J. C.; Chuluun-Erdene, E.; Esener, S.; Wang, J. Acoustic Droplet Vaporization and Propulsion of Perfluorocarbon-Loaded Microbullets for Targeted Tissue Penetration and Deformation. *Angew. Chem., Int. Ed.* **2012**, *51*, 7519−7522.
(45) Liu, J.; Yu, S.; Xu, B.; Tian, Z.; Zhang, H.; Liu, K.; Shi, X.; Zhao, Z.; Liu, C.; Lin, X.; Huang, G.; Solovev, A. A.; Cui, J.; Li, T.; Mei, Y. Magnetically Propelled Soft Microrobot Navigating Through Constricted Microchannels. *Appl. Mater. Today* **2021**, *25*, 101237.
(46) Zhao, H.; Hussain, A. M.; Duduta, M.; Vogt, D. M.; Wood, R. J.; Clarke, D. R. Compact Dielectric Elastomer Linear Actuators. *Adv. Funct. Mater.* **2018**, *28*, 1804328.

https://doi.org/10.1021/acs.chemmater.2c01960
Chem. Mater. 2022, 34, 9307−9328

(47) Herbert, R.; Lim, H. R.; Rigo, B.; Yeo, W. H. Fully Implantable Wireless Batteryless Vascular Electronics with Printed Soft Sensors for Multiplex Sensing of Hemodynamics. *Sci. Adv.* **2022**, *8*, No. eabm1175.
(48) Seuring, J.; Bayer, F. M.; Huber, K.; Agarwal, S. Upper Critical Solution Temperature of Poly(N-acryloyl glycinamide) in Water: A Concealed Property. *Macromolecules* **2012**, *45*, 374−384.
(49) Wei, Y.; Zeng, Q.; Hu, Q.; Wang, M.; Tao, J.; Wang, L. Self-Cleaned Electrochemical Protein Imprinting Biosensor Basing on a Thermo-Responsive Memory Hydrogel. *Biosens. Bioelectron.* **2018**, *99*, 136−141.
(50) Li, G.; Ma, Z.; You, C.; Huang, G.; Song, E.; Pan, R.; Zhu, H.; Xin, J.; Xu, B.; Lee, T.; An, Z.; Di, Z.; Mei, Y. Silicon Nanomembrane Phototransistor Flipped with Multifunctional Sensors Toward Smart Digital Dust. *Sci. Adv.* **2020**, *6*, No. eaaz6511.
(51) Shen, B.; Peng, W.; Su, B.; Wu, L.; Liu, Z.; Xu, H.; Zhao, J.; Feng, P.; Li, F. Elastic-Electric Coefficient-Sensitive Hydrogel Sensors toward Sweat Detection. *Anal. Chem.* **2022**, *94*, 1910−1917.
(52) Liu, X.; Yang, Y.; Inda, M. E.; Lin, S.; Wu, J.; Kim, Y.; Chen, X.; Ma, D.; Lu, T. K.; Zhao, X. Magnetic Living Hydrogels for Intestinal Localization, Retention, and Diagnosis. *Adv. Funct. Mater.* **2021**, *31*, 2010918.
(53) Larson, C.; Peele, B.; Li, S.; Robinson, S.; Totaro, M.; Beccai, L.; Mazzolai, B.; Shepherd, R. Highly Stretchable Electroluminescent Skin for Optical Signaling and Tactile Sensing. *Science* **2016**, *351*, 1071−1074.
(54) Zheng, M.; Wang, X.; Yue, O.; Hou, M.; Zhang, H.; Beyer, S.; Blocki, A. M.; Wang, Q.; Gong, G.; Liu, X.; Guo, J. Skin-Inspired Gelatin-Based Flexible Bio-Electronic Hydrogel for Wound Healing Promotion and Motion Sensing. *Biomaterials* **2021**, *276*, 121026.
(55) Battista, E.; Scognamiglio, P. L.; Di Luise, N.; Raucci, U.; Donati, G.; Rega, N.; Netti, P. A.; Causa, F. Turn-on Fluorescence Detection of Protein by Molecularly Imprinted Hydrogels Based on Supramolecular Assembly of Peptide Multi-Functional Blocks. *J. Mater. Chem. B* **2018**, *6*, 1207−1215.
(56) Wang, Y.; Huang, W.; Wang, Y.; Mu, X.; Ling, S.; Yu, H.; Chen, W.; Guo, C.; Watson, M. C.; Yu, Y.; Black, L. D., 3rd; Li, M.; Omenetto, F. G.; Li, C.; Kaplan, D. L. Stimuli-Responsive Composite Biopolymer Actuators with Selective Spatial Deformation Behavior. *Proc. Natl. Acad. Sci. U. S. A.* **2020**, *117*, 14602−14608.
(57) Li, J.; Ma, Q.; Xu, Y.; Yang, M.; Wu, Q.; Wang, F.; Sun, P. Highly Bidirectional Bendable Actuator Engineered by LCST-UCST Bilayer Hydrogel with Enhanced Interface. *ACS Appl. Mater. Interfaces* **2020**, *12*, 55290−55298.
(58) de Oliveira, T. E.; Mukherji, D.; Kremer, K.; Netz, P. A. Effects of Stereochemistry and Copolymerization on the LCST of PNIPAm. *J. Chem. Phys.* **2017**, *146*, 034904.
(59) Xia, M.; Cheng, Y.; Meng, Z.; Jiang, X.; Chen, Z.; Theato, P.; Zhu, M. A Novel Nanocomposite Hydrogel with Precisely Tunable UCST and LCST. *Macromol. Rapid Commun.* **2015**, *36*, 477−482.
(60) Zhang, S.; Elsayed, M.; Peng, R.; Chen, Y.; Zhang, Y.; Peng, J.; Li, W.; Chamberlain, M. D.; Nikitina, A.; Yu, S.; Liu, X.; Neale, S. L.; Wheeler, A. R. Reconfigurable Multi-Component Micromachines Driven by Optoelectronic Tweezers. *Nat. Commun.* **2021**, *12*, 5349.
(61) Li, C.; Iscen, A.; Palmer, L. C.; Schatz, G. C.; Stupp, S. I. Light-Driven Expansion of Spiropyran Hydrogels. *J. Am. Chem. Soc.* **2020**, *142*, 8447−8453.
(62) Moon, H. K.; Lee, S. H.; Choi, H. C. In Vivo Near-Infrared Mediated Tumor Destruction by Photothermal Effect of Carbon Nanotubes. *ACS Nano* **2009**, *3*, 3707−3713.
(63) Tong, X.; Zheng, J.; Lu, Y.; Zhang, Z.; Cheng, H. Swelling and Mechanical Behaviors of Carbon Nanotube/Poly(vinyl alcohol) Hybrid Hydrogels. *Mater. Lett.* **2007**, *61*, 1704−1706.
(64) Shin, S. R.; Jung, S. M.; Zalabany, M.; Kim, K.; Zorlutuna, P.; Kim, S. B.; Nikkhah, M.; Khabiry, M.; Azize, M.; Kong, J.; Wan, K. T.; Palacios, T.; Dokmeci, M. R.; Bae, H.; Tang, X. S.; Khademhosseini, A. Carbon-Nanotube-Embedded Hydrogel Sheets for Engineering Cardiac Constructs and Bioactuators. *ACS Nano* **2013**, *7*, 2369−2380.
(65) Xu, Y.; Sheng, K.; Li, C.; Shi, G. Self-Assembled Graphene Hydrogel via a One-Step Hydrothermal Process. *ACS Nano* **2010**, *4*, 4324−4330.
(66) Zhou, Y.; Hauser, A. W.; Bende, N. P.; Kuzyk, M. G.; Hayward, R. C. Waveguiding Microactuators Based on a Photothermally Responsive Nanocomposite Hydrogel. *Adv. Funct. Mater.* **2016**, *26*, 5447−5452.
(67) Li, M.; Wang, X.; Dong, B.; Sitti, M. In-Air Fast Response and High Speed Jumping and Rolling of a Light-Driven Hydrogel Actuator. *Nat. Commun.* **2020**, *11*, 3988.
(68) Tao, B.; Lin, C.; Deng, Y.; Yuan, Z.; Shen, X.; Chen, M.; He, Y.; Peng, Z.; Hu, Y.; Cai, K. Copper-Nanoparticle-Embedded Hydrogel for Killing Bacteria and Promoting Wound Healing with Photothermal Therapy. *J. Mater. Chem. B* **2019**, *7*, 2534−2548.
(69) Dong, Y.; Li, S.; Li, X.; Wang, X. Smart MXene/Agarose Hydrogel with Photothermal Property for Controlled Drug Release. *Int. J. Biol. Macromol.* **2021**, *190*, 693−699.
(70) Sun, Z.; Wei, C.; Liu, W.; Liu, H.; Liu, J.; Hao, R.; Huang, M.; He, S. Two-Dimensional MoO_2 Nanosheet Composite Hydrogels with High Transmittance and Excellent Photothermal Property for Near-Infrared Responsive Actuators and Microvalves. *ACS Appl. Mater. Interfaces* **2021**, *13*, 33404−33416.
(71) Kim, J. U.; Lee, S.; Kang, S. J.; Kim, T. I. Materials and Design of Nanostructured Broadband Light Absorbers for Advanced Light-to-Heat Conversion. *Nanoscale* **2018**, *10*, 21555−21574.
(72) Kim, J.; Chung, S. E.; Choi, S. E.; Lee, H.; Kim, J.; Kwon, S. Programming Magnetic Anisotropy in Polymeric Microactuators. *Nat. Mater.* **2011**, *10*, 747−752.
(73) Lum, G. Z.; Ye, Z.; Dong, X.; Marvi, H.; Erin, O.; Hu, W.; Sitti, M. Shape-Programmable Magnetic Soft Matter. *Proc. Natl. Acad. Sci. U. S. A.* **2016**, *113*, E6007−E6015.
(74) Du, X.; Cui, H.; Xu, T.; Huang, C.; Wang, Y.; Zhao, Q.; Xu, Y.; Wu, X. Reconfiguration, Camouflage, and Color-Shifting for Bio-inspired Adaptive Hydrogel-Based Millirobots. *Adv. Funct. Mater.* **2020**, *30*, 1909202.
(75) Yoshida, K.; Onoe, H. Soft Spiral-Shaped Microswimmers for Autonomous Swimming Control by Detecting Surrounding Environments. *Adv. Intell. Syst.* **2020**, *2*, 2000095.
(76) Brule, S.; Levy, M.; Wilhelm, C.; Letourneur, D.; Gazeau, F.; Menager, C.; Le Visage, C. Doxorubicin Release Triggered by Alginate Embedded Magnetic Nanoheaters: a Combined Therapy. *Adv. Mater.* **2011**, *23*, 787−790.
(77) Messing, R.; Schmidt, A. M. Perspectives for the Mechanical Manipulation of Hybrid Hydrogels. *Polym. Chem.* **2011**, *2*, 18−32.
(78) Ma, C.; Lu, W.; Yang, X.; He, J.; Le, X.; Wang, L.; Zhang, J.; Serpe, M. J.; Huang, Y.; Chen, T. Bioinspired Anisotropic Hydrogel Actuators with On-Off Switchable and Color-Tunable Fluorescence Behaviors. *Adv. Funct. Mater.* **2018**, *28*, 1704568.
(79) Spencer, A. R.; Primbetova, A.; Koppes, A. N.; Koppes, R. A.; Fenniri, H.; Annabi, N. Electroconductive Gelatin Methacryloyl-PEDOT:PSS Composite Hydrogels: Design, Synthesis, and Properties. *ACS Biomater. Sci. Eng.* **2018**, *4*, 1558−1567.
(80) Ye, T.; Wang, J.; Jiao, Y.; Li, L.; He, E.; Wang, L.; Li, Y.; Yun, Y.; Li, D.; Lu, J.; Chen, H.; Li, Q.; Li, F.; Gao, R.; Peng, H.; Zhang, Y. A Tissue-Like Soft All-Hydrogel Battery. *Adv. Mater.* **2022**, *34*, No. e2105120.
(81) Ohm, Y.; Pan, C.; Ford, M. J.; Huang, X.; Liao, J.; Majidi, C. An Electrically Conductive Silver-Polyacrylamide-Alginate Hydrogel Composite for Soft Electronics. *Nat. Electron.* **2021**, *4*, 185−192.
(82) Mishra, A. K.; Wallin, T. J.; Pan, W.; Xu, P.; Wang, K.; Giannelis, E. P.; Mazzolai, B.; Shepherd, R. F. Autonomic Perspiration in 3D-Printed Hydrogel Actuators. *Sci. Robot.* **2020**, *5*, No. eaaz3918.
(83) An, R.; Zhang, B.; Han, L.; Wang, X.; Zhang, Y.; Shi, L.; Ran, R. Strain-Sensitivity Conductive MWCNTs Composite Hydrogel for Wearable Device and Near-Infrared Photosensor. *J. Mater. Sci.* **2019**, *54*, 8515−8530.
(84) Shen, B.; Peng, W.; Su, B.; Wu, L.; Liu, Z.; Xu, H.; Zhao, J.; Feng, P.; Li, F. Elastic-Electric Coefficient-Sensitive Hydrogel Sensors toward Sweat Detection. *Anal. Chem.* **2022**, *94*, 1910−1917.

https://doi.org/10.1021/acs.chemmater.2c01960
Chem. Mater. 2022, 34, 9307−9328

(85) Kim, Y.; Yuk, H.; Zhao, R.; Chester, S. A.; Zhao, X. Printing Ferromagnetic Domains for Untethered Fast-Transforming Soft Materials. *Nature* **2018**, *558*, 274−279.
(86) Huang, T. Y.; Huang, H. W.; Jin, D. D.; Chen, Q. Y.; Huang, J. Y.; Zhang, L.; Duan, H. L. Four-Dimensional Micro-Building Blocks. *Sci. Adv.* **2020**, *6*, No. eaav8219.
(87) Eger, C. J.; Horstmann, M.; Poppinga, S.; Sachse, R.; Thierer, R.; Nestle, N.; Bruchmann, B.; Speck, T.; Bischoff, M.; Ruhe, J. The Structural and Mechanical Basis for Passive-Hydraulic Pine Cone Actuation. *Adv. Sci.* **2022**, *9*, 2200458.
(88) Huang, L.; Jiang, R.; Wu, J.; Song, J.; Bai, H.; Li, B.; Zhao, Q.; Xie, T. Ultrafast Digital Printing toward 4D Shape Changing Materials. *Adv. Mater.* **2017**, *29*, 1605390.
(89) Han, Z.; Wang, P.; Mao, G.; Yin, T.; Zhong, D.; Yiming, B.; Hu, X.; Jia, Z.; Nian, G.; Qu, S.; Yang, W. Dual pH-Responsive Hydrogel Actuator for Lipophilic Drug Delivery. *ACS Appl. Mater. Interfaces* **2020**, *12*, 12010−12017.
(90) Stoychev, G.; Zakharchenko, S.; Turcaud, S.; Dunlop, J. W.; Ionov, L. Shape-Programmed Folding of Stimuli-Responsive Polymer Bilayers. *ACS Nano* **2012**, *6*, 3925−3934.
(91) Luo, R.; Wu, J.; Dinh, N. D.; Chen, C. H. Gradient Porous Elastic Hydrogels with Shape-Memory Property and Anisotropic Responses for Programmable Locomotion. *Adv. Funct. Mater.* **2015**, *25*, 7272−7279.
(92) Breger, J. C.; Yoon, C.; Xiao, R.; Kwag, H. R.; Wang, M. O.; Fisher, J. P.; Nguyen, T. D.; Gracias, D. H. Self-Folding Thermo-Magnetically Responsive Soft Microgrippers. *ACS Appl. Mater. Interfaces* **2015**, *7*, 3398−3405.
(93) Kim, J.; Hanna, J. A.; Byun, M.; Santangelo, C. D.; Hayward, R. C. Designing Responsive Buckled Surfaces by Halftone Gel Lithography. *Science* **2012**, *335*, 1201−1205.
(94) Peng, X.; Liu, T.; Zhang, Q.; Shang, C.; Bai, Q.-W.; Wang, H. Surface Patterning of Hydrogels for Programmable and Complex Shape Deformations by Ion Inkjet Printing. *Adv. Funct. Mater.* **2017**, *27*, 1701962.
(95) Wang, Z. J.; Hong, W.; Wu, Z. L.; Zheng, Q. Site-Specific Pre-Swelling-Directed Morphing Structures of Patterned Hydrogels. *Angew. Chem., Int. Ed.* **2017**, *56*, 15974−15978.
(96) Ma, P.; Niu, B.; Lin, J.; Kang, T.; Qian, J.; Wu, Z. L.; Zheng, Q. Sequentially Controlled Deformations of Patterned Hydrogels into 3D Configurations with Multilevel Structures. *Macromol. Rapid Commun.* **2019**, *40*, No. e1800681.
(97) Wang, Z. J.; Zhu, C. N.; Hong, W.; Wu, Z. L.; Zheng, Q. Cooperative Deformations of Periodically Patterned Hydrogels. *Sci. Adv.* **2017**, *3*, No. e1700348.
(98) Timoshenko, S. Analysis of Bi-Metal Thermostats. *J. Opt. Soc. Am.* **1925**, *11*, 233−255.
(99) Li, S.; Wang, K. W. Plant-Inspired Adaptive Structures and Materials for Morphing and Actuation: A Review. *Bioinspir. Biomim.* **2017**, *12*, 011001.
(100) Armon, S.; Efrati, E.; Kupferman, R.; Sharon, E. Geometry and Mechanics in the Opening of Chiral Seed Pods. *Science* **2011**, *333*, 1726−1730.
(101) Sydney Gladman, A.; Matsumoto, E. A.; Nuzzo, R. G.; Mahadevan, L.; Lewis, J. A. Biomimetic 4D Printing. *Nat. Mater.* **2016**, *15*, 413−418.
(102) Kim, Y. S.; Liu, M.; Ishida, Y.; Ebina, Y.; Osada, M.; Sasaki, T.; Hikima, T.; Takata, M.; Aida, T. Thermoresponsive Actuation Enabled by Permittivity Switching in an Electrostatically Anisotropic Hydrogel. *Nat. Mater.* **2015**, *14*, 1002−1007.
(103) Wang, Z. J.; Zhu, C. N.; Hong, W.; Wu, Z. L.; Zheng, Q. Programmed Planar-to-Helical Shape Transformations of Composite Hydrogels with Bioinspired Layered Fibrous Structures. *J. Mater. Chem. B* **2016**, *4*, 7075−7079.
(104) Arslan, H.; Nojoomi, A.; Jeon, J.; Yum, K. 3D Printing of Anisotropic Hydrogels with Bioinspired Motion. *Adv. Sci.* **2019**, *6*, 1800703.
(105) Yuk, H.; Lin, S.; Ma, C.; Takaffoli, M.; Fang, N. X.; Zhao, X. Hydraulic Hydrogel Actuators and Robots Optically and Sonically Camouflaged in Water. *Nat. Commun.* **2017**, *8*, 14230.
(106) Meng, X.; Qiao, Y.; Do, C.; Bras, W.; He, C.; Ke, Y.; Russell, T. P.; Qiu, D. Hysteresis-Free Nanoparticle-Reinforced Hydrogels. *Adv. Mater.* **2022**, *34*, No. e2108243.
(107) Jia, H.; Mailand, E.; Zhou, J.; Huang, Z.; Dietler, G.; Kolinski, J. M.; Wang, X.; Sakar, M. S. Universal Soft Robotic Microgripper. *Small* **2019**, *15*, No. e1803870.
(108) Sun, Z.; Song, C.; Zhou, J.; Hao, C.; Liu, W.; Liu, H.; Wang, J.; Huang, M.; He, S.; Yang, M. Rapid Photothermal Responsive Conductive MXene Nanocomposite Hydrogels for Soft Manipulators and Sensitive Strain Sensors. *Macromol. Rapid Commun.* **2021**, *42*, No. e2100499.
(109) Qin, H.; Zhang, T.; Li, N.; Cong, H. P.; Yu, S. H. Anisotropic and Self-Healing Hydrogels With Multi-Responsive Actuating Capability. *Nat. Commun.* **2019**, *10*, 2202.
(110) Sun, Z.; Yamauchi, Y.; Araoka, F.; Kim, Y. S.; Bergueiro, J.; Ishida, Y.; Ebina, Y.; Sasaki, T.; Hikima, T.; Aida, T. An Anisotropic Hydrogel Actuator Enabling Earthworm-Like Directed Peristaltic Crawling. *Angew. Chem., Int. Ed.* **2018**, *57*, 15772−15776.
(111) Gao, G.; Wang, Z.; Xu, D.; Wang, L.; Xu, T.; Zhang, H.; Chen, J.; Fu, J. Snap-Buckling Motivated Controllable Jumping of Thermo-Responsive Hydrogel Bilayers. *ACS Appl. Mater. Interfaces* **2018**, *10*, 41724−41731.
(112) Ma, C.; Le, X.; Tang, X.; He, J.; Xiao, P.; Zheng, J.; Xiao, H.; Lu, W.; Zhang, J.; Huang, Y.; Chen, T. A Multiresponsive Anisotropic Hydrogel with Macroscopic 3D Complex Deformations. *Adv. Funct. Mater.* **2016**, *26*, 8670−8676.
(113) Ergene, E.; Liman, G.; Yildiz, E.; Yilgor Huri, P.; Demirel, G. Folding Control of Hydrogel Platforms through Pattern Design and Light Illumination. *ACS Appl. Polym. Mater.* **2021**, *3*, 3272−3277.
(114) Yin, C.; Wei, F.; Fu, S.; Zhai, Z.; Ge, Z.; Yao, L.; Jiang, M.; Liu, M. Visible Light-Driven Jellyfish-like Miniature Swimming Soft Robot. *ACS Appl. Mater. Interfaces* **2021**, *13*, 47147−47154.
(115) Jing, L.; Hsiao, L. Y.; Li, S.; Yang, H.; Ng, P. L. P.; Ding, M.; Truong, T. V.; Gao, S. P.; Li, K.; Guo, Y. X.; Valdivia, Y. A. P.; Chen, P. Y. 2D-Material-Integrated Hydrogels as Multifunctional Protective Skins for Soft Robots. *Mater. Horiz.* **2021**, *8*, 2065−2078.
(116) Zheng, S. Y.; Shen, Y.; Zhu, F.; Yin, J.; Qian, J.; Fu, J.; Wu, Z. L.; Zheng, Q. Programmed Deformations of 3D-Printed Tough Physical Hydrogels with High Response Speed and Large Output Force. *Adv. Funct. Mater.* **2018**, *28*, 1803366.
(117) Ma, M.; Guo, L.; Anderson, D. G.; Langer, R. J. S. Bio-inspired polymer composite actuator and generator driven by water gradients. *Science* **2013**, *339*, 186−189.
(118) Xiao, S.; Zhang, M.; He, X.; Huang, L.; Zhang, Y.; Ren, B.; Zhong, M.; Chang, Y.; Yang, J.; Zheng, J. Dual Salt- and Thermoresponsive Programmable Bilayer Hydrogel Actuators with Pseudo-Interpenetrating Double-Network Structures. *ACS Appl. Mater. Interfaces* **2018**, *10*, 21642−21653.
(119) Hua, M.; Wu, D.; Wu, S.; Ma, Y.; Alsaid, Y.; He, X. 4D Printable Tough and Thermoresponsive Hydrogels. *ACS Appl. Mater. Interfaces* **2021**, *13*, 12689−12697.
(120) Kaynak, M.; Dirix, P.; Sakar, M. S. Addressable Acoustic Actuation of 3D Printed Soft Robotic Microsystems. *Adv. Sci.* **2020**, *7*, 2001120.
(121) Wang, H.; Gu, X.; Wang, C. Self-Propelling Hydrogel/Emulsion-Hydrogel Soft Motors for Water Purification. *ACS Appl. Mater. Interfaces* **2016**, *8*, 9413−9422.
(122) Son, H.; Byun, E.; Yoon, Y. J.; Nam, J.; Song, S. H.; Yoon, C. Untethered Actuation of Hybrid Hydrogel Gripper via Ultrasound. *ACS Macro Lett.* **2020**, *9*, 1766−1772.
(123) Zhang, J.; Zeng, L.; Qiao, Z.; Wang, J.; Jiang, X.; Zhang, Y. S.; Yang, H. Functionalizing Double-Network Hydrogels for Applications in Remote Actuation and in Low-Temperature Strain Sensing. *ACS Appl. Mater. Interfaces* **2020**, *12*, 30247−30258.
(124) Hua, L.; Xie, M.; Jian, Y.; Wu, B.; Chen, C.; Zhao, C. Multiple-Responsive and Amphibious Hydrogel Actuator Based on Asymmetric

https://doi.org/10.1021/acs.chemmater.2c01960
Chem. Mater. 2022, 34, 9307−9328

UCST-Type Volume Phase Transition. *ACS Appl. Mater. Interfaces* **2019**, *11*, 43641−43648.
(125) Cole, L. *Biology of Life: Biochemistry, Physiology and Philosophy*; Academic Press, 2016; pp 1−184.
(126) Illeperuma, W. R. K.; Sun, J. Y.; Suo, Z.; Vlassak, J. J. Force and Stroke of a Hydrogel Actuator. *Soft Matter* **2013**, *9*, 8504−8511.
(127) Horváth, J. Chemomechanical Oscillations with a Non-Redox Non-Oscillatory Reaction. *Chem. Commun.* **2017**, *53*, 4973−4976.
(128) He, X.; Aizenberg, M.; Kuksenok, O.; Zarzar, L. D.; Shastri, A.; Balazs, A. C.; Aizenberg, J. Synthetic Homeostatic Materials With Chemo-Mechano-Chemical Self-Regulation. *Nature* **2012**, *487*, 214−218.
(129) Shin, B.; Ha, J.; Lee, M.; Park, K.; Park, G. H.; Choi, T. H.; Cho, K. J.; Kim, H. Y. Hygrobot: A Self-Locomotive Ratcheted Actuator Powered by Environmental Humidity. *Sci. Robot.* **2018**, *3*, No. eaar2629.
(130) Zhao, Y.; Xuan, C.; Qian, X.; Alsaid, Y.; Hua, M.; Jin, L.; He, X. Soft Phototactic Swimmer Based on Self-Sustained Hydrogel Oscillator. *Sci. Robot.* **2019**, *4*, No. eaax7112.
(131) Wang, X.; Qin, X. H.; Hu, C.; Terzopoulou, A.; Chen, X. Z.; Huang, T. Y.; Maniura-Weber, K.; Pané, S.; Nelson, B. J. 3D Printed Enzymatically Biodegradable Soft Helical Microswimmers. *Adv. Funct. Mater.* **2018**, *28*, 1804107.
(132) Lata, J. P.; Guo, F.; Guo, J.; Huang, P. H.; Yang, J.; Huang, T. J. Surface Acoustic Waves Grant Superior Spatial Control of Cells Embedded in Hydrogel Fibers. *Adv. Mater.* **2016**, *28*, 8632−8638.
(133) Dillinger, C.; Nama, N.; Ahmed, D. Ultrasound-Activated Ciliary Bands for Microrobotic Systems Inspired by Starfish. *Nat. Commun.* **2021**, *12*, 6455.
(134) Xu, T.; Xu, L. P.; Zhang, X. Ultrasound Propulsion of Micro-/Nanomotors. *Appl. Mater. Today* **2017**, *9*, 493−503.
(135) Ahmed, D.; Lu, M.; Nourhani, A.; Lammert, P. E.; Stratton, Z.; Muddana, H. S.; Crespi, V. H.; Huang, T. J. Selectively Manipulable Acoustic-Powered Microswimmers. *Sci. Rep.* **2015**, *5*, 9744.
(136) Wang, W.; Castro, L. A.; Hoyos, M.; Mallouk, T. E. Autonomous Motion of Metallic Microrods Propelled by Ultrasound. *ACS Nano* **2012**, *6*, 6122−6132.
(137) Kaynak, M.; Ozcelik, A.; Nourhani, A.; Lammert, P. E.; Crespi, V. H.; Huang, T. J. Acoustic Actuation of Bioinspired Microswimmers. *Lab Chip* **2017**, *17*, 395−400.
(138) Ma, Y.; Hua, M.; Wu, S.; Du, Y.; Pei, X.; Zhu, X.; Zhou, F.; He, X. Bioinspired High-Power-Density Strong Contractile Hydrogel by Programmable Elastic Recoil. *Sci. Adv.* **2020**, *6*, No. eabd2520.
(139) Keller, S.; Teora, S. P.; Hu, G. X.; Nijemeisland, M.; Wilson, D. A. High-Throughput Design of Biocompatible Enzyme-Based Hydrogel Microparticles with Autonomous Movement. *Angew. Chem., Int. Ed.* **2018**, *57*, 9814−9817.
(140) Yu, Y.; Shang, L.; Gao, W.; Zhao, Z.; Wang, H.; Zhao, Y. Microfluidic Lithography of Bioinspired Helical Micromotors. *Angew. Chem., Int. Ed.* **2017**, *56*, 12127−12131.
(141) Zhu, W.; Li, J.; Leong, Y. J.; Rozen, I.; Qu, X.; Dong, R.; Wu, Z.; Gao, W.; Chung, P. H.; Wang, J.; Chen, S. 3D-Printed Artificial Microfish. *Adv. Mater.* **2015**, *27*, 4411−4417.
(142) Laocharoensuk, R.; Burdick, J.; Wang, J. Carbon-Nanotube-Induced Acceleration of Catalytic Nanomotors. *ACS Nano* **2008**, *2*, 1069−1075.
(143) Abdelmohsen, L. K. E. A.; Nijemeisland, M.; Pawar, G. M.; Janssen, G.-J. A.; Nolte, R. J. M.; van Hest, J. C. M.; Wilson, D. A. Dynamic Loading and Unloading of Proteins in Polymeric Stomatocytes: Formation of an Enzyme-Loaded Supramolecular Nanomotor. *ACS Nano* **2016**, *10*, 2652−2660.
(144) Solovev, A. A.; Mei, Y.; Schmidt, O. G. Catalytic Microstrider at the Air-Liquid Interface. *Adv. Mater.* **2010**, *22*, 4340−4344.
(145) Hansen-Bruhn, M.; de Avila, B. E.; Beltran-Gastelum, M.; Zhao, J.; Ramirez-Herrera, D. E.; Angsantikul, P.; Vesterager Gothelf, K.; Zhang, L.; Wang, J. Active Intracellular Delivery of a Cas9/sgRNA Complex Using Ultrasound-Propelled Nanomotors. *Angew. Chem., Int. Ed.* **2018**, *57*, 2657−2661.
(146) Peng, X.; Li, J.; Lin, L.; Liu, Y.; Zheng, Y. Opto-Thermophoretic Manipulation and Construction of Colloidal Superstructures in Photocurable Hydrogels. *ACS Appl. Nano Mater.* **2018**, *1*, 3998−4004.
(147) Tu, Y.; Peng, F.; Sui, X.; Men, Y.; White, P. B.; van Hest, J. C. M.; Wilson, D. A. Self-Propelled Supramolecular Nanomotors with Temperature-Responsive Speed Regulation. *Nat. Chem.* **2017**, *9*, 480−486.
(148) Zhang, L.; Xiao, Z.; Chen, X.; Chen, J.; Wang, W. Confined 1D Propulsion of Metallodielectric Janus Micromotors on Microelectrodes under Alternating Current Electric Fields. *ACS Nano* **2019**, *13*, 8842−8853.
(149) Liu, J.; Chen, H.; Shi, X.; Nawar, S.; Werner, J. G.; Huang, G.; Ye, M.; Weitz, D. A.; Solovev, A. A.; Mei, Y. Hydrogel Microcapsules with Photocatalytic Nanoparticles for Removal of Organic Pollutants. *Environ. Sci.: Nano* **2020**, *7*, 656−664.
(150) Hao, J.; Yang, W.; Zhang, Z.; Tang, J. Surfactant-Assisted Fabrication of 3D Prussian Blue-Reduced Graphene Oxide Hydrogel as a Self-Propelling Motor for Water Treatment. *Nanoscale* **2015**, *7*, 10498−10503.
(151) Ma, S.; Thiele, J.; Liu, X.; Bai, Y.; Abell, C.; Huck, W. T. Fabrication of Microgel Particles With Complex Shape Via Selective Polymerization of Aqueous Two-Phase Systems. *Small* **2012**, *8*, 2356−2360.
(152) Chen, C. H.; Abate, A. R.; Lee, D.; Terentjev, E. M.; Weitz, D. A. Microfluidic Assembly of Magnetic Hydrogel Particles with Uniformly Anisotropic Structure. *Adv. Mater.* **2009**, *21*, 3201−3204.
(153) Zhu, H.; Nawar, S.; Werner, J. G.; Liu, J.; Huang, G.; Mei, Y.; Weitz, D. A.; Solovev, A. A. Hydrogel Micromotors with Catalyst-Containing Liquid Core and Shell. *J. Phys.: Condens. Matter* **2019**, *31*, 214004.
(154) Wang, Z.; Fu, D.; Xie, D.; Fu, S.; Wu, J.; Wang, S.; Wang, F.; Ye, Y.; Tu, Y.; Peng, F. Magnetic Helical Hydrogel Motor for Directing T Cell Chemotaxis. *Adv. Funct. Mater.* **2021**, *31*, 2101648.
(155) Wu, J.; Liu, L.; Chen, B.; Ou, J.; Wang, F.; Gao, J.; Jiang, J.; Ye, Y.; Wang, S.; Tong, F.; Tian, H.; Wilson, D. A.; Tu, Y.; Peng, F. Magnetically Powered Helical Hydrogel Motor for Macrophage Delivery. *Appl. Mater. Today* **2021**, *25*, 101197.
(156) Soto, F.; Karshalev, E.; Zhang, F.; Esteban Fernandez de Avila, B.; Nourhani, A.; Wang, J. Smart Materials for Microrobots. *Chem. Rev.* **2022**, *122*, 5365−5403.
(157) Huang, H. W.; Sakar, M. S.; Petruska, A. J.; Pane, S.; Nelson, B. J. Soft Micromachines with Programmable Motility and Morphology. *Nat. Commun.* **2016**, *7*, 12263.
(158) Huang, H. W.; Uslu, F. E.; Katsamba, P.; Lauga, E.; Sakar, M. S.; Nelson, B. J. Adaptive Locomotion of Artificial Microswimmers. *Sci. Adv.* **2019**, *5*, No. eaau1532.
(159) Zhang, L.; Abbott, J. J.; Dong, L.; Kratochvil, B. E.; Bell, D.; Nelson, B. J. Artificial Bacterial Flagella: Fabrication and Magnetic Control. *Appl. Phys. Lett.* **2009**, *94*, 064107.
(160) Magdanz, V.; Khalil, I. S. M.; Simmchen, J.; Furtado, G. P.; Mohanty, S.; Gebauer, J.; Xu, H.; Klingner, A.; Aziz, A.; Medina-Sanchez, M.; Schmidt, O. G.; Misra, S. IRONSperm: Sperm-Templated Soft Magnetic Microrobots. *Sci. Adv.* **2020**, *6*, No. eaba5855.
(161) Tottori, S.; Zhang, L.; Qiu, F.; Krawczyk, K. K.; Franco-Obregon, A.; Nelson, B. J. Magnetic Helical Micromachines: Fabrication, Controlled Swimming, and Cargo Transport. *Adv. Mater.* **2012**, *24*, 811−816.
(162) Geim, A.; Simon, M.; Boamfa, M.; Heflinger, L. J. N. Magnet Levitation at Your Fingertips. *Nature* **1999**, *400*, 323−324.
(163) Kummer, M. P.; Abbott, J. J.; Kratochvil, B. E.; Borer, R.; Sengul, A.; Nelson, B. J. OctoMag: An Electromagnetic System for 5-DOF Wireless Micromanipulation. *IEEE Trans. Robot.* **2010**, *26*, 1006−1017.
(164) Fusco, S.; Sakar, M. S.; Kennedy, S.; Peters, C.; Bottani, R.; Starsich, F.; Mao, A.; Sotiriou, G. A.; Pane, S.; Pratsinis, S. E.; Mooney, D.; Nelson, B. J. An Integrated Microrobotic Platform for On-Demand, Targeted Therapeutic Interventions. *Adv. Mater.* **2014**, *26*, 952−957.
(165) Llacer-Wintle, J.; Rivas-Dapena, A.; Chen, X. Z.; Pellicer, E.; Nelson, B. J.; Puigmarti-Luis, J.; Pane, S. Biodegradable Small-Scale

https://doi.org/10.1021/acs.chemmater.2c01960
Chem. Mater. 2022, 34, 9307−9328

Swimmers for Biomedical Applications. *Adv. Mater.* **2021**, *33*, No. e2102049.
(166) Cabanach, P.; Pena-Francesch, A.; Sheehan, D.; Bozuyuk, U.; Yasa, O.; Borros, S.; Sitti, M. Zwitterionic 3D-Printed Non-Immunogenic Stealth Microrobots. *Adv. Mater.* **2020**, *32*, No. e2003013.
(167) Sun, H. C. M.; Liao, P.; Wei, T.; Zhang, L.; Sun, D. Magnetically Powered Biodegradable Microswimmers. *Micromachines* **2020**, *11*, 404.
(168) Gervasoni, S.; Terzopoulou, A.; Franco, C.; Veciana, A.; Pedrini, N.; Burri, J. T.; de Marco, C.; Siringil, E. C.; Chen, X. Z.; Nelson, B. J.; Puigmarti-Luis, J.; Pane, S. CANDYBOTS: A New Generation of 3D-Printed Sugar-Based Transient Small-Scale Robots. *Adv. Mater.* **2020**, *32*, No. e2005652.
(169) Pena-Francesch, A.; Giltinan, J.; Sitti, M. Multifunctional and Biodegradable Self-Propelled Protein Motors. *Nat. Commun.* **2019**, *10*, 3188.
(170) Terzopoulou, A.; Wang, X.; Chen, X. Z.; Palacios-Corella, M.; Pujante, C.; Herrero-Martin, J.; Qin, X. H.; Sort, J.; deMello, A. J.; Nelson, B. J.; Puigmarti-Luis, J.; Pane, S. Biodegradable Metal-Organic Framework-Based Microrobots (MOFBOTs). *Adv. Healthc. Mater.* **2020**, *9*, No. e2001031.
(171) Chen, W.; Chen, X.; Yang, M.; Li, S.; Fan, X.; Zhang, H.; Xie, H. Triple-Configurational Magnetic Robot for Targeted Drug Delivery and Sustained Release. *ACS Appl. Mater. Interfaces* **2021**, *13*, 45315−45324.
(172) Scriven, L. E.; Sternling, C. V. The Marangoni Effects. *Nature* **1960**, *187*, 186−188.
(173) Sharma, R.; Chang, S. T.; Velev, O. D. Gel-Based Self-Propelling Particles Get Programmed to Dance. *Langmuir* **2012**, *28*, 10128−10135.

https://doi.org/10.1021/acs.chemmater.2c01960
Chem. Mater. 2022, 34, 9307−9328